Ternary SnSb-ZnO nano-composite as a potential anode material for high energy density Lithium-ion Battery

A DISSERTATION

SUBMITTED IN PARTIAL FULFILLMENT OF THE REQUIREMENTS

FOR THE AWARDS OF THE DEGREE

OF

MASTER OF TECHNOLOGY

IN

NANO SCIENCE AND TECHNOLOGY

Submitted by:

SAUMYA

2K16/NST/08

Under the supervision of

DR. AMRISH K. PANWAR

DEPARTMENT OF APPLIED PHYSICS

DELHI TECHNOLOGICAL UNIVERSITY
(Formerly Delhi College of Engineering)
Bawana Road, Delhi-110042

JUNE 2018

DELHI TECHNOLOGICAL UNIVERSITY
(Formerly Delhi College of Engineering)
Bawana Road, Delhi-110042

CANDIDATE'S DECLARATION

I, Saumya, Roll No. 2K16/NST/08 of M.Tech. (Nano Science and Technology), hereby declare that the project Dissertation titled "Ternary SnSb-ZnO nano-composite as a potential anode material for high energy density Lithium-ion Battery" which is submitted by me to the Department of Applied Physics, Delhi Technological University, Delhi in partial fulfillment of the requirement for the award of the degree of Master of Technology, is original and not copied from any source without proper citation. This work has not formed the basis for the award of any Degree, Diploma, Associateship, Fellowship or other similar title or recognition.

Place: Delhi **SAUMYA**

Date: **2K16/NST/08**

M.Tech- NST

DEPARTMENT OF APPLIED PHYSICS
DELHI TECHNOLOGICAL UNIVERSITY
(Formerly Delhi College of Engineering)
Bawana Road, Delhi-110042

CERTIFICATE

I hereby certify that the Project Dissertation titled "**Ternary SnSb-ZnO nano-composite as a potential anode material for high energy density Lithium-ion Battery**" which is submitted by Saumya, Roll No. 2K16/NST/08, Department of Applied Physics, Delhi Technological University, Delhi in partial fulfillment of the requirement for the award of the degree of Master of Technology, is a record of the project work carried out by the students under my supervision. To the best of my knowledge this work has not been submitted in part or full for any Degree or Diploma to this University or elsewhere.

Dr. Amrish K. Panwar **Prof. Suresh. C. Sharma**

Supervisor **Head of Department**

ACKNOWLEDGEMENT

With great pleasure I would like to express my first and sincere gratitude to my supervisor Dr. Amrish K. Panwar for his continuous support, patience, motivating ideas, enthusiasm and immense knowledge. His guidance has always enlightened and helped me to shape and develop my work.

Besides my supervisor, I would like to express my deep gratitude and respect to Prof. S. C. Sharma, Head, Department of Applied Physics, Delhi Technological University, Delhi for his encouragement, insightful comments and valuable suggestion during the course.

I wish to extend my thanks to Mr. Abhishek Bharadwaj, Ms. Snigdha Sharma and Ms. Shivangi Rajput for their help, cooperation, advice and assistance in keeping my progress on schedule. I am highly obliged for their valuable and constructive suggestions during the planning and development of this research work.

I would also like to thank my friends Manish Kumar and Astha Srivastava for keeping me motivated throughout the project working and development, and extend my gratitude towards my family for their goodwill and support that helped me a lot in successful completion of this project.

Saumya
2K16/NST/08
Nano Science & Technology

Table of Content

List of Figures

List of Tables

ABSTRACT

Novel ternary Sn-Sb-ZnO nano-composites were synthesized using mechanochemical activation technique. Lithium ion batteries (LIBs) have drawn pervasive attention in compact devices and hybrid electric vehicles because of their high-power density along with enhanced levels of energy density. Alloy type anode materials, especially anode materials which are based on or form compounds with Sn- and Sb- have presented themselves as a possible and sustainable replacement of graphite. Lithium forms alloy with elements Sn and Sb. The resulting compounds were examined and the theoretical specific capacities of "$Li_{4.4}Sn$" and "Li_3Sb" were found nearly to be equal to 991 mAh/g and 660 mAh/g, respectively. When metallic tin (Sn) attains the state of full lithiation i.e. $Li_{4.4}Sn$, its theoretical capacity has been found to reach 990 mAh g^{-1}. This makes a wide range of tin based compounds to be considered as potential anode material. Antimony being a close neighbor of Sn is also a potential anode material in the rudimentary form, as well as when it forms compounds. The lithiation/delithiation in antimony speeds up at a relatively low values of voltage range. Nano-sized Sn-Sb, when effectively used as an anode material can gain the advantages while overcoming the associated disadvantage of volume expansion problem with SnSb based anode materials.

CHAPTER 1

INTRODUCTION

1.1. Background

One of the most important elements in the energy and electricity sector is the storage of energy. Ever since our encounter with electricity, we have sought efficient approaches to store the energy for use as per our needs. Over the last era, the energy storage industry has progressed and become acquainted to the requirements of ever changing energy and advancement in technology. The technology of storing and reusing the energy broadly covers some major areas that differ in power and energy requirements. Energy storage could be described as the process to remit an amount of the energy that is produced, for use at a later time, either as final energy or by converting into more stable forms. Energy storage is significant for the advancement and integration of renewable energy technologies, to deliver increased consistency, to stabilize minor instabilities in yield of energy for minor as well as extensive generations, development of efficient commutation systems like trains and bikes and even electric vehicles. Such systems also prove to be very cost effective. Several distinctive forms of electricity storage have come into existence, the most common being, battery, compressed air, pumped hydro and flywheel [1].

1.2. Battery

"A collection of cell or cell assemblies is known as battery". A cell is an electrochemical unit which comprises of a negative electrode, a positive electrode, a separator, and an electrolyte. Electricity is said to be generated due to a series of chemical reactions which take place because of involvement of chemical species of the electrodes and electrolyte. Therefore, "any device which is capable of generating electrical energy by transforming chemical energy can be defined as a battery". The electrons move from the negative terminal in the direction of the positive terminal, under the condition of an external load connected across the battery, which results in generation of an electric current. This current is used to power a light bulb, computer, electric vehicles, clocks, mobile phones, and several other electronic devices [2]. A battery is unable to produce electricity if the electrode material is completely consumed as the electrons may no more be available. As a result only, a limited amount of power may be available in the battery. However, a variety of batteries can be refurbished by altering the course of flow of electrons by means of a different source of power. The reversal of electrochemical processes inside the battery, restore the positive and the negative electrode to their original state and the battery can be used again.

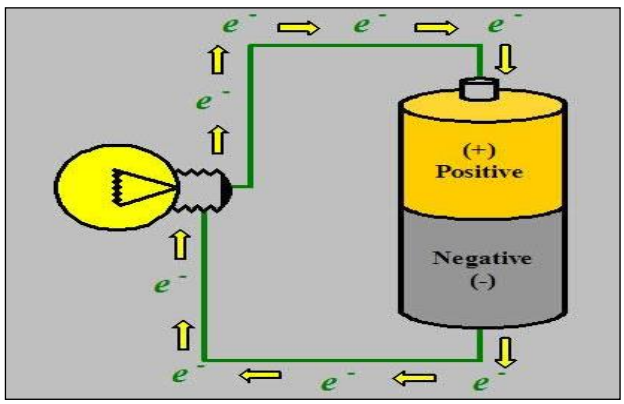

Figure 1.1. Working principle of a Battery [1]

1.2.1. History of Rechargeable Batteries

In 1859, the idea of the first rechargeable (aka secondary) battery was conceived by Gaston Planté, a French physicist. The first lead acid cell prototype included sulfuric acid and a reel of two sheets of lead. Passage of reverse current through it results in the restoration of the reaction mechanism. In 1881, the design was improved by Camille Alphonso Faure by replacing the spiral sheet by plates. A plate was formed by devising a network of lead, embedded with lead oxide. This steered easy manufacture and wide-spread use into automobile industry [3].

In 1970's, Nickel-hydrogen battery were developed by "COMSAT for communication satellites". A variant of nickel-hydrogen battery, nickel-metal hydride (NiMH) batteries came into existence in the later years. In 1989 the consumer market welcomed the rechargeable batteries, which proved to be an affordable and smaller alternative to nickel-hydrogen cells. In 1912, G.N. Lewis experimented with Lithium batteries and they struck the market in 1970. The first Lithium-ion battery was developed by Asahi Chemical of Japan. Lithium-ion battery is rechargeable and is more stable adaptation of Lithium battery. In 1991, commercialization of the first Lithium-ion battery was done by Sony. Lithium polymer battery were introduced in 1997, which stored the electrolyte in a solid polymer composite [4].

Figure 1.2. A modern-day Lithium-ion Battery [4]

1.3. Lithium-ion Battery

Being the lightest metal in the periodic table, Lithium possesses highest electrochemical potential and delivers largest specific energy per weight. "Although using Lithium metal as an anode in the rechargeable batteries provided extraordinarily high energy densities, unwanted dendrites growth on anode during cycling became a major issue with such batteries, as it resulted into electrical short." With the volatility of metallic lithium, the research studies provided a solution using "Lithium-ion". When Sony commercialized the first "Lithium-ion battery" in 1991, "Lithium-ion battery" became the fastest growing battery in the industry.

Lithium-ion battery are most commonly used in consumer and home electronics. Even though their specific energy is lower than the Lithium-metal, they are safer when used within the specified limits of voltage and current ratings. Over the years, the manufacturing cost for Lithium-ion battery has decreased with increase in its capacity. The cost effectiveness, increased specific energy and, the absence of toxic elements has made Li-ion the most desirable rechargeable battery for portable applications, satellite application, heavy industries and electric vehicles. Also, when paralleled to other batteries under same category, such as nickel-cadmium or nickel-metal hydride, "Lithium-ion batteries don't suffer from memory effect, show minimal self-discharge (5-10%) and, have very high energy density." Lithium-ion batteries possess a theoretical voltage of 4.1V and practical voltage of 3.7V with a longer life period (2000+ cycles) compared to nickel-cadmium (1.2V, 500 cycles) and nickel-metal hydride (1.4V, 600 cycles) [5].

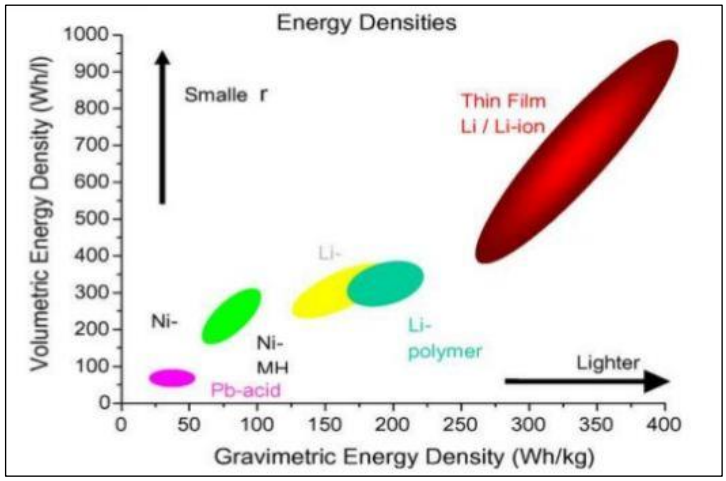

Figure 1.3. Energy density of different rechargeable batteries [5]

1.3.1. History of Lithium-ion Battery

Due to safety concern with metallic Lithium electrodes, research to develop the batteries which used lithium compounds were present began. In 1974-76, Besenhard, discovered and proposed "the application of reversible intercalation in graphite and intercalation in cathodic oxides". Samar Basu's experiment demonstrating intercalation of lithium in graphite, resulted in development of LiC_6 electrode at Bell labs in 1977. In 1979, John B. Goodenough invented the Lithium-cobalt-oxide battery. "This battery used $LiCoO_2$ as the positive electrode and lithium metal as the negative electrode." This laid the foundation to the prospects of using stable and efficient materials as negative electrodes instead of Lithium-metal as lithium-cobalt-oxide acts as a donor of Lithium-ions. A variety of ternary compounds, such as $LiMn_2O_4$, $LiMnO_3$, Lithium-copper-oxide and Lithium-nickel-oxide, were also identified along with lithium-cobalt-oxide in the later years. Rashid Yazami explained the reversible lithiation in graphite using a solid electrolyte. These graphite electrodes discovered by "Yazami" are the universally accepted electrodes used in Li-ion batteries. In 1983, "John. B. Goodenough and coworkers" exploited manganese spinel as a promising positive electrode for lithium-ion batteries. The use of spinel electrodes in commercial batteries started from the year 2013. The prototype cell using $LiCoO_2$ as the positive electrode and a carbon rich material in which

lithium ions could be fitted was assembled in 1985. John Goodenough also established that higher voltages could be achieved when poly-anions such as sulfates are used as the positive electrodes. “The first commercial Lithium-ion battery was introduced by Sony and Asahi Kasei in 1991”. Over the years, $LiFePO_4$, lithium-metal phosphates (olivine), lithium-nickel-manganese-cobalt-oxide and several other materials were recognized to be successfully implemented as positive electrodes. In recent years, graphite as the anode material has also been replaced by silicon, Lithium-titanate (LTO), tin/cobalt alloys etc. There are several ongoing researches to find low voltage anode materials without compromising the energy stored per unit volume. “The current global lithium-ion battery production capacity is marked at 28 GWh” [6-10].

1.3.2. Construction of a Lithium-ion battery

Like any standard battery, a lithium-ion battery is also composed of a positive electrode, a negative electrode, electrolyte, separators and casings. The positive electrode in a conventional lithium-ion battery is a metal-oxide such as $LiCoO_2$. The negative electrode consists of porous carbon (commonly graphite) and the electrolyte is a lithium salt dissolved in organic solvent (usually 1:2 EC: DMC: $LiPF_6$). The electrochemical characteristics of the electrodes reverse between the anode and the cathode conditional to the current direction. The separator used is usually a micro perforated sheet of plastic which prevents the positive and the negative electrodes to come in contact and allows ions to pass through it. The outer case is made of metal which comes with a pressure sensitive vent because of the pressurized battery [11-12].

1.3.3. Electrochemistry

Lithium-ions move in and out of the electrodes through the process called intercalation/insertion (lithiation) and de-intercalation/extraction (de-lithiation). “When the battery undergoes charging, the positively charged lithium ions move

from the positive electrode towards the negative electrode through the electrolyte while the electrons move in the same direction via an external circuit". Implantation of these lithium ions in the negative electrode occurs by a process known as lithiation or intercalation. While discharging, oxidation at the negative electrode occurs and the electrons and lithium-ions move towards the positive electrode via an external circuit and electrolyte, respectively. This process of removal of lithium ions is known as de-intercalation. While discharging, oxidation, defined as the electrons loss, occurs at the negative terminal while reduction which may be defined as electron benefit occurs at the positive terminal. This passage of positive ions from anode to the cathode causes a current to flow within the circuit. Similarly, charging results in oxidation at the positive terminal and reduction at the negative terminal and the applied over-voltage induces a charging current within the circuit [13-15].

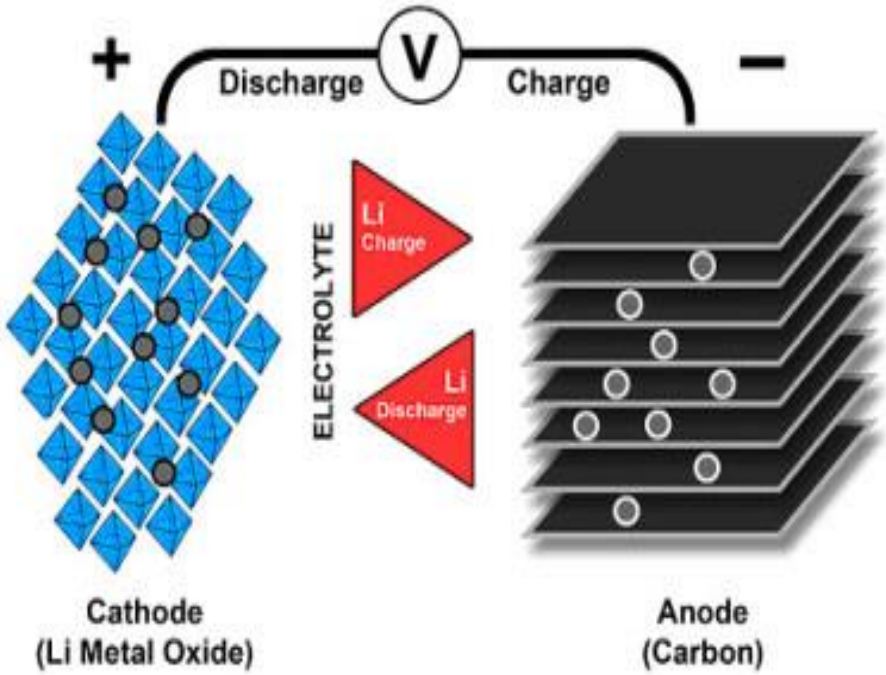

Figure 1.4. Ion flow in lithium-ion battery [15]

The positive electrode reaction is:

$$CoO_2 + Li^+ + e^- \rightleftharpoons LiCoO_2$$

The negative electrode reaction is:

$$LiC_6 \rightleftharpoons C_6 + Li^+ + e^-$$

The overall reaction occurring in a Lithium-ion battery

$$LiC_6 + CoO_2 \rightleftharpoons C_6 + LiCoO_2$$

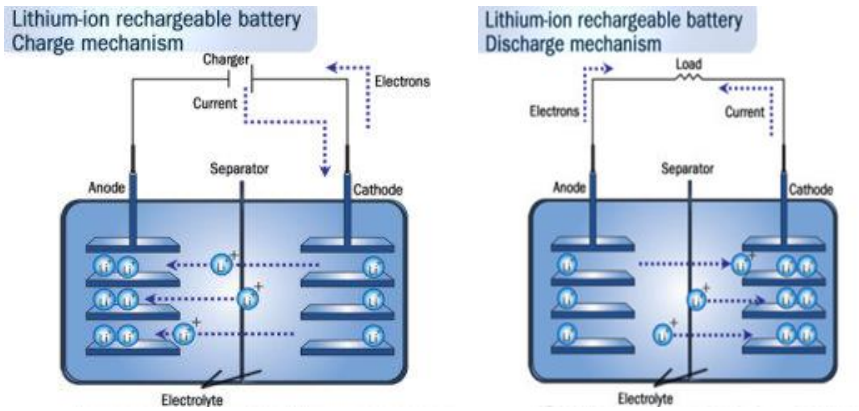

(a) **(b)**

Figure 1.5. (a) Charging and, (b) discharging mechanism in a Li-ion Battery [14]

Even with excellent rechargeable properties, lithium-ion batteries suffer from various losses during the first intercalation/de-intercalation process. Formation of solid electrolyte interface (SEI) during the first charging and discharging is considered to be one of the major losses that occurs in the Li-ion batteries. This SEI coating forms due to "interaction between the electrode materials and the electrolyte". It provides electrical insulation, and increased ionic conductivity and also prevents intercalation of solvent into the electrode. Lithium-oxide, lithium-fluoride, and semi-carbonates together constitute the SEI.

1.3.4. Electrode materials

The materials that fulfil the criteria of having good electrical conductivity, decent ionic conductivity, reversible capacity, long cycle life, high diffusion rate, cost effective, and non-toxic, are considered as suitable electrode material for lithium-ion batteries [16].

- **Cathode**

A desired cathode material for a lithium-ion battery is the one which has "a high discharge capacity, high energy capacity, long cycle life, high power density, low self-discharge, sufficiently high voltage and non-hazardous".

The first layered transition metal oxide cathode to be discovered was $LiCoO_2$ by John B. Goodenough and continue to be used in most of the commercial Li-ion batteries [17]. With cobalt and lithium ions occupying alternate layers of octahedral sites and cubic closed packed oxygen atoms, the compound has a hexagonal symmetry. $LiCoO_2$ (LCO) has a very high and desired theoretical volumetric capacity of 1363 mAh cm^{-3}. Additionally, it also possesses a specific capacity (theoretical) of 274 mAh g^{-1}. It also possesses other desirable characteristics such as superior cycling performance, more voltage discharge and reduced self-discharging. LCO has a sloping potential profile in lithium half cells and below the voltage of 4.2V vs. Li/Li^+, almost lithium ions are partly removed which results in high specific capacity [18, 19]. Higher capacities could be attained using LCO as a cathode material but it also steers structural instability due to de-intercalated Li_xCoO_2. Being a limited resource, cobalt costs very high and this makes LCO cathodes expensive. LCO cathodes also possess lowest thermal stability compared to other transition metal oxide cathodes. At a low temperature of over 200°C, LCO cathodes suffer from thermal runaway due to exothermic reactions between organic materials and released oxygen. This sets a limitation on the use of LCO as the cathode material [20].

Table 1.1. Specific capacity, volumetric capacity and average potentials of Intercalation cathode materials [20]

Crystal Structure	Compound	Volumetric capacity (mAh cm^{-3})	Specific capacity (mAh g^{-1})	Average Voltage (V)
Layered	$LiTiS_2$	697	225/210	1.9
	$LiCoO_2$	1363	274/148	3.8
	$LiNiO_2$	1280	275/150	3.8
	$LiMnO_2$	1148	285/140	3.3
	$LiNi_{0.33}Co_{0.33}Mn_{0.33}O_2$	1333	280/160	3.7
	$LiNi_{0.8}Co_{0.15}Al_{0.05}O_2$	1284	279/199	3.7
	Li_2MnO_3	1708	458/180	3.8
Spinel	$LiMn_2O_4$	596	148/120	4.1
	$LiCo_2O_4$	704	142/84	4.0
Olivine	$LiFePO_4$	589	170/165	3.4
	$LiMnPO_4$	567	171/168	3.8
	$LiCoPO_4$	510	167/125	4.2
Tavorite	$LiFeSO_4F$	487	151/120	3.7
	$LiVPO_4F$	484	156/129	4.2

- **Anode**

Lithium metal, despite of highest capacity (3860 mAh g^{-1}), is not preferred as an anode material because of dendrite formation leading to short circuit, thermal runaway, and other safety issues. Several efforts have been made to develop suitable anode materials with enhanced energy and power density which also deliver high capacity, long cycle life, and ease of lithium-ion diffusion [21, 22]. Carbon based materials such as, carbon nanotubes (CNT), graphene, porous carbon etc. have been probed for high capacity and improved performances. Non-carbon materials that have been investigated as anode for secondary batteries include silicon oxide (SiO), silicon (S), germanium (Ge), tin (Sn), and transition metal oxides. The major limitations for selection of anode materials

are poor electron transport, capacity fading, high volume expansion and minimal value of coulombic efficiency. These limitations are overcome by nano-structuring the aforementioned materials for effective use as anode [23-25].

Incorporation of nanotechnology in development of lithium-ion batteries results in substantial increase in capacity and elevated flux of lithium-ion across electrolyte and electrode interface. Reduction to nanoscale from bulk, leads to increased surface area which provides lithium storage at more functional sites and lithium diffusion rate increases due to decreased path length. The various innovative anode materials can be categorized into following types [26]:

(a) Intercalation and de-intercalation materials (carbon based materials, titanium dioxide, and LTO)

(b) Alloy and de-alloy materials such as Si, Sn, Al, and SnO_2

(c) Conversion materials such as transition metal oxides, metal sulfides, metal phosphides, and metal nitrides.

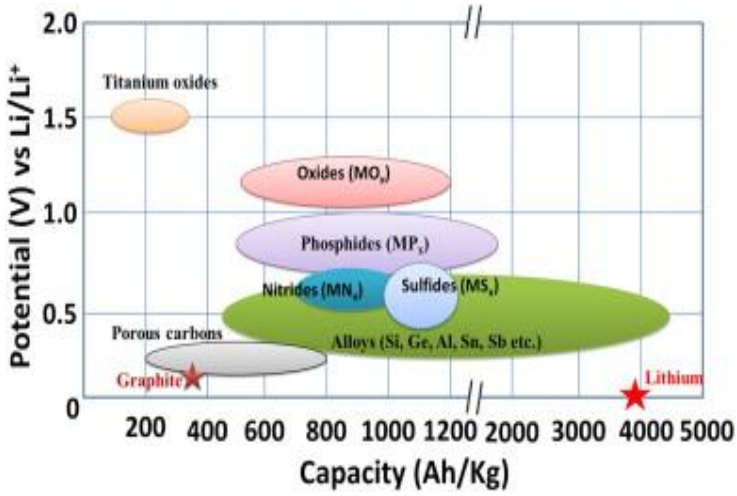

Figure 1.6. Variation in capacity density and average discharge potentials of various anode materials [26]

a. *Intercalation/de-intercalation materials*

Due to their good reversibility of lithium intercalation/de-intercalation, abundance in nature, stability in electrochemical and thermal environment, carbonaceous anode became commercially viable almost two decades ago. Since carbon displays electrical and chemical activity towards electrolytic solution at very low value of potentials, carbon coating on active materials prevent the active electrode material degradation as well as capacity fade upon charging and discharging and lessens the electrolyte's decomposition producing a thinner solid electrolyte interface film over the electrode [27]. Being chemically stable, carbon coating provides protection against HF corrosion and surface oxidation in case of nanostructured active materials. When graphite is carbon coated, it reduces the degradation of electrolyte and does not allow any electrolyte species to intercalate into the graphene layers. Similarly, carbon coating the LTO electrodes, helps reduce electrolyte decomposition. For silicon and germanium anodes, carbon coating led to improved battery performances [28, 29].

In carbon based materials, a single Li-ion intercalates with carbon atoms, six in number, resulting into a lithiated compound LiC_6. Carbon based materials can be categorized into two types: soft carbon (graphitic) and hard carbon. In graphitic carbons, unidirectional piling of the crystallites is observed where as in hard carbons, they have a disordered orientation. With large graphite grains, soft carbons can attain their theoretical capacity (372 mAh g^{-1}). But due to the low value of the reversible capacity, they have their application limited to low power devices such as mobiles and laptops etc. [30, 31]. The major drawback of using graphitic carbon as an anode material is that propylene carbonate (electrolyte) tends to intercalate along with the Li-ions and causes exfoliation and capacity fading. Also during lithium insertion, graphitic carbon experience strain in their crystal structure which results in decreasing the cycle life of the cell. Surface coating with amorphous carbon helps achieve superior coloumbic efficiency. The various commercially available graphites are Massive Artificial Graphite (MAG), Mesocarbon Microbead (MCMB), and carbon fiber-vapor

grown (VGCF) etc. Development of nano-fibers, porous carbon, CNT, and graphene as a suitable carbon derived anode material is under research. These materials are expected to impart novel properties and increase the energy storage capacity of the secondary batteries [32, 33].

Hard carbons having disordered orientation tend not to undergo exfoliation upon lithiation. Compared to the soft carbon they possess much higher theoretical capacity (500 mAh g^{-1}) in the potential range 1.5V vs. Li/Li^{+}. Due to random alignment of graphene sheets in hard carbon, nanovoids are present in between them which permits reduced and identical volume expansion in every direction. However, these voids lead to slow diffusion of Li-ions and thus inferior rate capacity. Low tap density and initial coulombic efficiency are considered to be the major drawbacks associated with hard carbon anodes. Coating of hard carbon with a fine film of metal film or soft carbon improves the coloumbic efficiency and the capacity to store lithium. Enhanced rate capability (~ $4.11x10^{-5}$ cm^2 s^{-1}) and cycle life were observed when nano-porous hard carbon materials were synthesized [34-36].

Carbon nanotubes (CNT) when used in association with other active anode materials, produce superior results because of their extraordinary thermal and mechanical stability, adsorption, electronic conductivity, and transport properties. SWNT's can achieve theoretical capacity reaching up to 1163 mAh g^{-1} for LiC_2 compound. This is because the lithium ion diffuses into stable surface sites of quasi graphitic layers, as well as within the tube. Certain nanostructured materials or oxides (M_xO_y: M = Cr, Mo, Mn, Cu, Ni, and Fe) when coupled with carbon nanotubes, improve the serviceability of the battery and its storage capacity of the lithium ions. Synthesis of such hybrid anode materials result in CNT's which reduces the changes in volume observed during the discharge cycle and charge cycle processes. Fan et al. stated that "CNT's with a coating of Fe_3O_4 displayed a capacity of 800 mAh g^{-1} for 100 charge/ discharge cycles and also improved rate capability" [37].

With superior properties like high mechanical strength, high values of charge mobility and surface area, along with good electrical conductivity it makes a very significant anode material to be used in Li-ion batteries. When several layers of graphene is taken into account, the amount of absorbed lithium is significantly huge and therefore, and as a consequence the capacity associated with the Li_2C_6 stoichiometry is 780 mAh g^{-1} and 1116 mAh g^{-1} with LiC_2. Li_2C_6 is formed when lithium ion interacts and get absorbed on both the faces of the graphene sheets. LiC_2 results when lithium is trapped in a covalent bond of a benzene ring. Pan et al. reported graphene sheets synthesized using low temperature pyrolysis, reduction process of hydrazine and electron beam irradiation. The graphene sheets when when analyzed electrochemically established and displayed high gravimetric capacity ranging from 790 to 1050 mAh g^{-1}. Nano ribbons developed from MWNT's also possess lithium storage capability with capacity reaching a maximum of 800 mAh g^{-1}. Several research activities have suggested that use of graphene/metal, or graphene/metal phosphides/sulfides/oxides and semiconductors results into composites with reduced volume changes and excellent battery performance with capacity of 1220-1600 mAh g^{-1} [38].

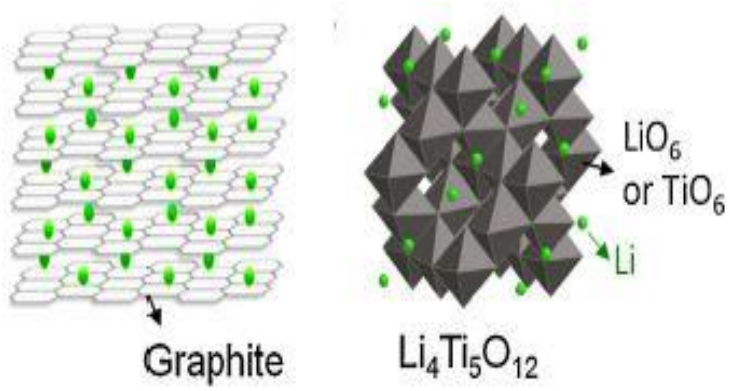

Figure 1.7. Crystal structure of lithiated graphite and LTO

Another important intercalation/de-intercalation anode material are titanium based oxides i.e. Lithium titanium oxide (LTO/ $Li_4Ti_5O_{12}$) and titania (TiO_2). These most important characteristics of these materials which make them suitable anode materials are inexpensive, non-toxic, nominal volume change upon charging and discharging and extended cycle life. Compared to their counterparts they have low theoretical capacity and electrical conductivity. However, with size reduced to nanoscale, these materials show improved capacity, longer cycle life, and efficient rate capability. LTO experiences 'zero strain' intercalation mechanism which is the main reason of stability of these anodes. Lithiation/de-lithiation in LTO anodes causes very small volume change as a result they are considered to be 'zero strain' materials. The SEI formation in LTO anodes is also inhibited because of the high equilibrium potential voltage of ~1.55V vs. Li/Li^+ that permits the operation marginally above 1V. LTO anodes are also considered to be tremendously safe. The cause for its high potential prevents Li dendrite formation. Consequently, they are considered suitable for high power, low energy and high cycle life lithium-ion batteries [39, 40].

Table 1.2. Comparison of characteristics of different anode materials [40]

Material	D ($cm^2\ s^{-1}$)	De-lithiation potential (V)	Lithiation potential (V)	Volume change
Graphite	10^{-11}-10^{-7}	0.1, 0.14, 0.23	0.07, 0.10, 0.19	10 %
LTO	10^{-12}-10^{-11}	1.58	1.55	0.2 %
Silicon	10^{-13}-10^{-11}	0.34, 0.57	0.05, 0.21	270 %
Germanium	10^{-12}-10^{-10}	0.5, 0.62	0.2, 0.3	240 %
Tin	10^{-16}-10^{-13}	0.58, 0.7, 0.78	0.4, 0.69	255 %
Li_2O	$5x10^{-12} – 5x10^{-10}$	N/A	N/A	N/A

b. *Alloy/de-alloy materials*

To satisfy the exigency of devices consuming high energy, electric vehicles (EV's), HEV's and other stationary applications, extensive research studies are

being carried out to develop improved and new materials for anodes with elevated values of specific capacity. The materials that are considered to provide for the high requirement of specific capacity include, silicon (Si), germanium (Ge), silicon monoxide (SiO), tin oxide (SnO), which participate in reaction with lithium via alloy/de-alloy mechanism [41]. Several metals are also found to be reactive towards lithium according to alloying/de-alloying mechanism such as, Al, Mg, Sb, Zn, Pb, Pt, Au, Cd Ag, and Ge etc. However, just silicon, tin, antimony, aluminum, and magnesium have been widely examined for research as they are inexpensive, abundant in nature and non-toxic. Pure metals, alloys or intermetallic are capable to be anode materials [42].

The theoretical capacities for silicon is as high as 4200 mAh g^{-1} and for oxides of tin (SnO_2 and SnO) it is 990 mAh g^{-1}. However, alloy anodes suffer from massive volume change upon lithium intercalation which results in short cycle life. The volume expansion and contraction also causes particle fracture and loss of electrical contact. It is also found that the volume change in the alloy anode materials may cause depletion of SEI layer and thereby increases the cell impedance due to electrolyte decay. Recent research studies examined the shortcomings and provided several elucidations which proved to be helpful in development of efficient alloy anode materials. The most useful strategies include downsizing the material particles to nano scale and synthesis of composites with lithium active/inactive materials [43].

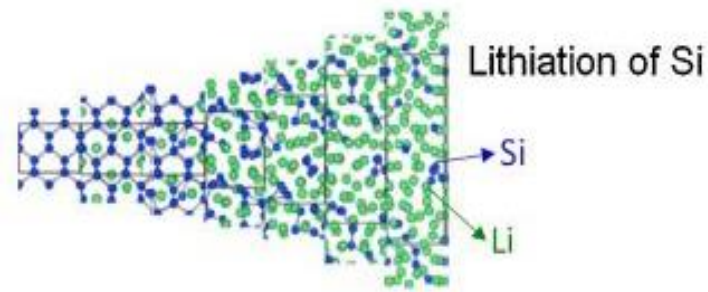

Figure 1.8. Crystal structure of Silicon during lithiation

Silicon happens to be the second highly abundant and eco-friendly element on earth and is thought to be the most valuable material for anodes to be used in future generation of Li-ion batteries. Silicon has the highest theoretical specific and volumetric capacity. The formation of Li-Si binary intermetallic is the reason behind the high specific capacity of silicon anodes. Another reason for silicon to be considered an effective anode material is due to the low de-lithiation potential and chemical stability. The problems associated with volume change such as low cycle life, destruction of SEI protective layer and irreversibility of lithium insertion/extraction can be overcome by use of silicon nanowires, nanotubes, and nanospheres. These nanostructures provide sufficient space for accommodation of volume growth during alloying as well as during the de-alloying process. This, in return, stabilizes the SEI and prevents the coalescing of particles enabling longer cycle life [44]. This led to development of anodes with remarkable electrochemical performances with experimental specific capacity reaching up to 3500 mAh g^{-1}. Silicon nanotubes and nano-wires have exhibited reversible capacity more than 2000 mAh g^{-1} with improved cycling performances. Also, the enhanced theoretical capacity greater than 1600 mAh g^{-1}, makes SiO_2 a desirable choice for anode material for lithium-ion batteries.

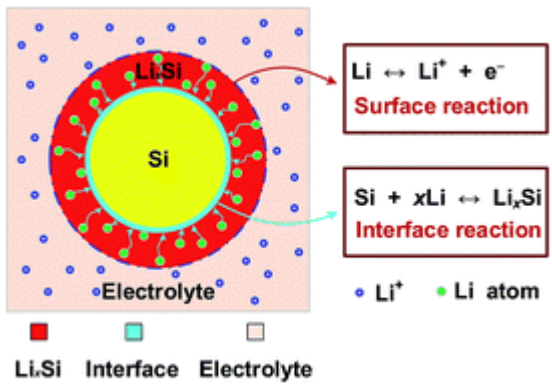

Figure 1.9. Lithiation/de-lithiation in Silicon anode for lithium-ion batteries

"Tin and tin oxide are also considered to be important anode materials with high theoretical specific capacity of 990 mAh g^{-1} and 783 mAh g^{-1} respectively".

However, they also undergo electrode degradation resulting from severe volume expansion over several cycles. Several attempts have been made to improve the irreversible capacity loss and to increase the cycling stability of tin and tin-oxide. Synthesis of nanostructures and nanocomposites is one such solution which helps to contain the large variation in the volume during lithiation/de-lithiation. Yin et al. suggested that "use of mesoporous SnO_2 spheres showed improved battery performance with capacity 761 mAh g^{-1} at a current density of 200 mAg^{-1} and 483 mAh g^{-1} at 2000 mAg^{-1}". Further developments were reported with the use of carbon composites such as SnO2/carbon nanoparticles, SnO_2/CNT's, SnO_2 (carbon-coated) and SnO_2/graphene [45-47].

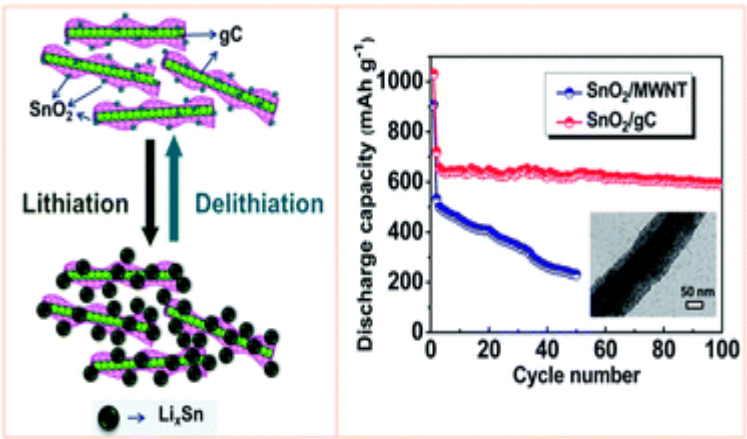

Figure 1.10. Lithiation/ de-lithiation mechanism in Tin oxide and the graph of its charge/discharge capacity [45]

Other alloy materials such as germanium, gallium, and aluminum have been considered to be efficient as anode materials. Ge does not suffer from particle fracture but is expensive for large scale industrial use. Zinc, lead and cadmium have high volumetric capacities but inferior specific capacity. Antimony, even though toxic, possess high specific capacity and results in superior battery performance.

c. *Conversion materials*

The conversion material comprises of transition metal compound in the form M_xN_y (N: Oxides, phosphides, nitrides or sulfides). When utilized in anode for lithium-ion batteries, these compounds undergo redox reactions beside composition and decomposition of lithium compounds (Li_xN_y). Such compounds demonstrate reversible capacities between 500-1200 mAh g^{-1} as a result of high electron transport [48].

"Iron based oxides, haematite (Fe_2O_3) and magnetite (Fe_3O_4) have high theoretical capacities, 1007 mAh g^{-1} and 926 mAh g^{-1} respectively". They are considered to be appropriate anode material because their non-toxicity, low cost and abundance in the nature. Several research works concentrating on development of new and different techniques for fabrication of iron oxide particles with size in nano dimension, which do not suffer from volume expansion, low lithium diffusion and iron accumulation. It was reported that structural integrity, with improved chemical kinetics and power capability were achieved using carbon based composited of iron oxides as well as by carbon coating these oxides. Excellent electrochemical performances of porous iron oxide (Fe_2O_3) nanotubes have indicated that conductive carbon composites of iron oxides can be a suitable substitute for graphite anodes [49]. Similarly, cobalt oxides and their porous nanostructures have indicated excellent cycling performances, enhanced lithium storage capacity and good rate capability. The theoretical capacity for Co_3O_4 was discovered to be 890 mAh g^{-1} and 715 mAh g^{-1} for CoO. Composites of cobalt oxides have been exploited in the research works to study buffering action in response to the volume changes and also to inhibit the extrication and coagulation of material oxides during processes of lithium intercalation/ de-intercalation [50].

Other materials which have extensively been probed for the application as anode materials include metals, phosphides, sulfides, and nitrides. Iron, tin,

nickel, antimony, and tungsten have drawn a lot of attention because of their lithium storage potential and structural integrity during lithiation/de-lithiation. These compounds participate with lithium via conversion reaction as well as intercalation/de-intercalation reaction. Then again, the commercialization of these materials across the Li-ion battery market is still in the pipeline due to the high potential hysteresis and poor retention of the capacity. It is, hence, viable that anodes with high energy and power densities need to be fabricated with inexpensive approaches for large scale production of nanomaterials [51].

Table 1.3. A comparative study of commonly used anode materials for Li-ion battery [51]

Active anode material	**Theoretical capacities (mAh g^{-1})**	**Comments**
Insertion/de-insertion Materials		
Hard Carbon	200-600	**Advantages:** Fine working potential, reduced cost, increased level of safety **Issues:** Low coulombic efficiency**,** high hysteresis in voltage**,** high irreversible capacity
CNT	1116	
Graphene	780/1116	
$LiTi_4O_5$	175	**Advantages:** Extreme safety, good cycle life, low cost, high power capability **Issues:** Very low capacity, low energy density
LiO_2	330	
Alloy/de-alloy Materials		
Si	4212	**Advantages:** High capacities, high energy density, good safety
Ge	1624	
Sn	993	
Sb	660	

SnO_2	790	**Issues:** Large irreversible capacity, huge capacity fading, poor cycling
SiO	1600	
Conversion Materials		
Metal oxides (Fe_2O_3, Fe_3O_4, CoO, Co_3O_4, Mn_xO_y, etc.)	500-1200	**Advantages:** High capacity, high energy, low cost **Issues:** Low columbic efficiency, unstable SEI, large hysteresis
Metal phosphides/ sulfides/nitrides	500-1800	**Advantages:** High specific capacity, low polarization than counter oxides **Issues:** Poor retention of capacity, expensive

1.3.5. Electrolyte

Electrolytes with high purity content are one of the most essential component of Li-ion battery system. The lithium-ions are carried from cathode to anode and vice-versa via electrolyte. Liquid electrolytes comprise an organic solvent in which a salt of lithium, such as $LiBF_4$, $LiPF_6$ or $LiClO_4$, is dispersed. The solvents which are organic in nature are ethylene carbonate (EC), di-ethyl carbonate (DEC), and di-methyl carbonate (DMC). $LiPF_6$ dissolved in ethylene carbonate together with a linear carbonate such as DEC, DMC and ethyl methyl carbonate (EMC), is the most important and common electrolyte. $LiPF_6$ is preferred because it acts as a passivizing agent and protects the current collector (Al) for cathode. Ethylene carbonate provides high ionic conductivity and the linear carbonated (DEC and DMC) help in decreasing the viscosity of the electrolyte as well as in easy penetration into polyolefin-based separators. The presence of organic solvents help in the creation of solid electrolyte interface (SEI), which acts as a protective layer on the surface of the negative electrode. EMC is thermally most compatible with ethylene carbonate. A mixture of EC/EMC forms a binary solvent which helps in achieving low liquidus

temperature with high ionic conductivity. Compared to DEC and DMC, ethyl methyl carbonate shows more stability towards cathode, lithium metal or lithium inserted compounds. The conductivity of a liquid electrolytes at room temperature is observed to be 0.1 S/m which increases with increase in temperature (30-40% increase at 40° C). POE (poly (oxyethylene)) based electrolytes provide a steady interface whereas RTILs can aid in regulating the combustibility and instability of organic electrolytes [52, 53].

Latest research in battery technology are aimed at exploring the use of solid material, such as ceramic, as an electrolyte. These ceramics are lithium metal oxides which exhibit better lithium transport with no risk of spillage. Solid electrolytes can be of two types: Ceramics and glassy. Solid ceramic electrolytes have highly ordered structure crystal structure with ion transport channels. Glassy electrolytes are amorphous in nature with higher conductivity. Common examples of ceramic electrolyte are pervoskites and lithium super ion conductors (LISICON). The conductivity of solid electrolytes vary in the range 10^{-4} – 10^{-1} S/m.

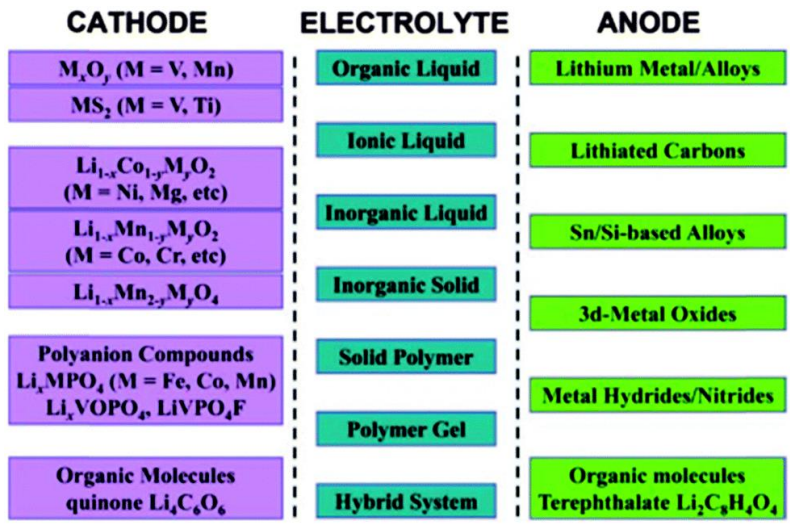

Figure 1.11. Representative electrode materials and electrolyte types investigated for Lithium-ion batteries.

With ever advancing technology, numerous research works are being carried out to develop more efficient Li-ion batteries. Several strategies have been developed to enable the application of novel electrode materials including modification of the electrolytes. The strategies such as composite formation, encapsulation and coating, morphology control allow faster ion and electron transport, surface reactivity, increased mechanical stability, improved chemical and thermal stability, prevention of electrolyte decomposition and stabilization of surface reactions. As seen in fig 1.18, several comprehensive studies of various electrodes illustrating their average electrode potential versus theoretical specific capacity have been conducted over the years. Such research works have helped to identify various cathode and anode combinations, electrolytes, separators, and current collectors for choice of material of electrodes [54].

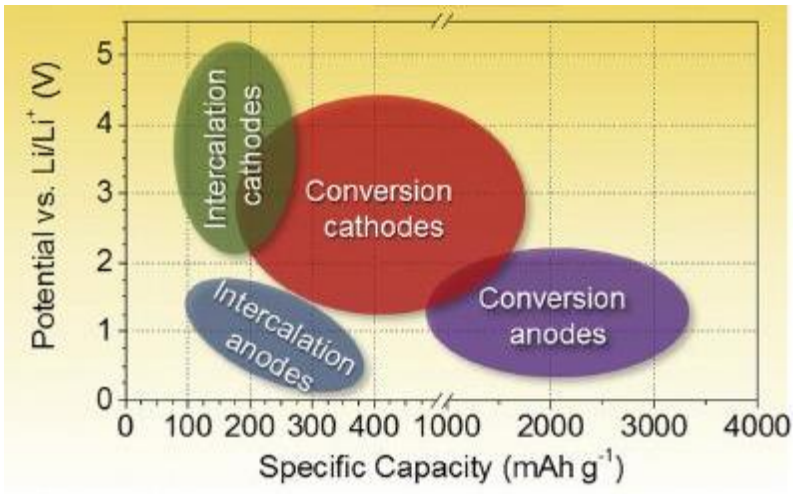

Figure 1.12. An summary of the mean specific capacities and discharge potentials for varieties of electrodes. [54]

Their high capacity, high power density and low pollution, makes lithium-ion batteries a promising contender for future energy strategies. Efficient, light-weight and high energy storing batteries are being developed for its applications ranging smart phones, computers to large capacity for EVs and HEVs, common applications in day-to-day life.

1.3.6. Advantages and Disadvantages of Li-ion battery

Lithium-ion batteries have gained popularity due to their advantages over other competing technologies [55].

1. Compared to other rechargeable batteries, Li-ion batteries are lighter in weight for the same size of battery. Being a reactive element, lithium stores great amount of energy in the bonds of its atomic structure. As a result, these batteries have high energy density. A nickel-metal hydride battery can hold 60-70 w-h per kilograms of power while a typical Li-ion battery stores 150 watt-hours/kg.
2. The self-discharge rates of these batteries is quite lower than that of Ni-MH and Ni-Cd batteries.
3. They do not suffer from memory effect, as a result they need not be discharged completely before charging again.
4. Li-ion batteries undergo hundreds of charge/ discharge cycles.
5. Lithium-ion batteries show longer cycle life and show lower effective capacity loss at high discharge rates.
6. Lithium-ion batteries can be charged much quickly and also possess higher open-circuit voltage than other secondary batteries.

Despite several advantages, lithium-ion batteries are associated with a few disadvantages as well [56]:

1. Lithium-ion batteries are expensive to manufacture compared to secondary batteries. The onboard circuitry involved with lithium-ion batteries to manage current and voltage within specified limits increase the overall cost of these batteries.
2. Lithium-ion batteries also suffer from aging effect, which means it starts degrading as soon as it leaves the factory. This implies that even with longer charge/discharge cycles, they are not quite durable.

3. When overcharged or overheated, lithium-ion batteries tend to explode. Ignition of electrolyte and fire risks may occur due to overheating or internal short circuit.
4. In its completely discharged state a LIB is entirely ruined and are susceptible to high values of temperature.

1.4. Scope of the thesis

The work mentioned in this dissertation illustrates the selection of a suitable alloy based anode materials for development of high energy Li-ion battery. The selected material was SnSb because of their high theoretical specific capacities and columbic efficiency. ZnO was used as a dopant to prevent the agglomeration of the particles which in turn prevents volume expansion observed in bare SnSb alloys based anodes. The active material was synthesized using solid state reaction method which involves high-energy ball milling. Physical characterizations that were conducted include, X-ray diffraction, scanning electron microscopy and energy dispersive spectroscopy. Electrochemical tests involving CV tests and electrochemical impedance spectroscopy.

CHAPTER 2

LITERATURE REVIEW

Over the past few decades there has been humongous research work in the development of Lithium-ion battery. Sundry experiments aimed at improving its energy density, safety, and cycle durability have put us closer to the accomplishment of the goal to fabricate and produce energy storage devices which are much more reliable, safer and environment friendly. Following are some significant research work which discuss the various advances in the field.

J. Yang, M. Winter and J.O. Besenhard (1996) significantly improved "the cycling performance of Li-alloy anodes (M + Li+ + e- LixM) in secondary organic electrolyte based lithium batteries by substituting compact particle size metal matrices M(e.g. Sn or Sb) with small particle size (micro- or nano-scale) multiphase metallic host materials like Sn/SnSbx or Sn/SnAgx". They deduced that the cycling performance of Li-ion batteries significantly is contingent up on the morphology of the matrix material. It was found that the volume expansion during lithiation occurred with the absence of major cracks. They established that the reason for such an effect was that the more reactive phase was embedded and allowed to expand in the lesser reactive phase [57].

Yong Wang et al. (2006) published a report unfolding the synthesis of bimetallic Sn–Sb nanorods in CNT templates. The Sn–Sb nanorods encapsulated within CNT, revealed high specific capacities and good cyclability when verified as the anode of lithium-ion batteries. The size scaling to nano dimensions and the rod-like morphology resulted in improved specific capacities and stable cycling performance. They also illustrated that the presence of CNT provided good electrical and mechanical stability as well as hindered the coagulation of molten SnSb vapors. The fabrication technique and the resulting improvements laid the foundation of using similar methods for similar low Li-alloying metals such as Sn-Cu, Sn-Fe, and Sn-Ni etc. [58].

Zhong Wang et al. (2007) synthesized Sn-Sb ultrafine particles with varying compositions and also investigated their structure, morphology, size and chemical composition. Consistent results were obtained after physical and chemical characterization of the synthesized materials. Spherical particles were observed with average particles size in the range of 100-300 nm. It was observed that the crystal structure of the materials is dependent on the proportion of the master alloy. In this study, the sample with 46.5% of Sn content showed best electrochemical results with highest reversible li-ion storage capacity (701 mAh g^{-1}) which stabilized at 566 mAh g^{-1} after 20 cycles. As an alternative anode material β-SnSb have capacity retention and superior reversible capacity [59].

Yude Wang et al. (2009) synthesized antimony doped tin oxide (SnO_2) nanoparticles by a polymer-assisted sol-gel process. The characterization results verified that the ATO nanopowders formed were highly crystalline in nature and that the antimony particles were contained in the SnO_2 crystal structure. The as-synthesized products displayed an initial "discharge capacity of 2400 mAh g^{-1} at current rate of C/5". Stable capacity of 637 mAh g^{-1} was obtained after 100 cycles. Wang et al. explained that the obvious aggregation of metallic tin toward larger entities was reduced because of the nanostructuring the materials. Size

reduction also accounts for the accommodation of the change in volume of the tin during Li alloying/dealloying. As a matter of fact, it was also established that along with providing higher surface area, nanostructured ATO facilitated the diffusion of electrolytes and Li-ions and provided the added advantage of mechanical reversibility of charging-discharging changes [60].

Hong Li, Zhaoxiang Wang, Liquan Chen, and Xuejie Huang (2009) reviewed the topical progress devoted to the anode and the cathode materials that have the capability to achieve the decisive factors of cost, safety, lifetime, durability, power density, and energy density. In their investigation of nanostructured inorganic compounds. The review extensively discusses the effect of size and morphology on the lithium storage potential of carbon-based materials, alloy anodes and conversion materials. The study also revealed that the use of nano/micro core-shell, surface pinning and dispersed composite structure have effectively improved the cycling operation of the Li-ion batteries. The importance of surface coating of cathode materials leading in thermal and chemical stability have been brought in attention. The review paper also put forward the future requirements for development of efficient, safe and eco-friendly lithium-ion batteries. It underlines the future significance of the integration strategies deliberating the electrode materials, electrode structure and the electrode/electrolyte interface. Investigation of electron and ion transport, particularly in $LiFePO_4$ using theoretical simulations and experiments, revealed that presence of dopants in the lattice of $LiFePO_4$, may be successful approach to increase its electronic conductivity and reduce blockage of Li-ion transport along 1D channel [61].

Shuangqiang Chen et al. (2010) reported the preparation and lithium storage property of graphene supported SnSb@carbon and SnSb nanoparticles. The mixed phase peaks were observed and confirmed via X-Ray diffraction technique and the morphology was studied via SEM analysis which affirms the

uniform distribution of particles as was expected. Higher initial charge capacities were observed in GNS-supported Sn–Sb nanoparticles and Sn–Sb@carbon. The excellent lithium storage properties and the cycling rate are ascribed to the carbon coating on the SnSb composite and support provided by GNS [62].

Wei-Jun Zhang (2011) studied and reviewed the recent progress in improving and understanding the electrochemical performance of various alloy anodes. In this study, he summarizes the different approaches used for performance improvement of lithium-ion batteries, and deliberates the causes of first-cycle irreversible capacity loss. A comparison of irreversible capacity loss and capacity retention is provided. In his review, he highlighted that incorporation of carbon matrix composites resulted in the best performance of alloy anode materials. He also emphasized that use of binder and electrolyte also determine the cycle life and capacity retention [63].

Ali Reza Kamali and Derek J. Fray (2011) reviewed the increasing importance of application of Tin based materials for application as anode in lithium-ion batteries with improved energy storage and with increased capacity. The microstructures and production processes of different tin-based anode materials were discussed in the review paper. Several tin-based intermetallics and their composites were also discussed. Due to the need for cost effectiveness and industry scalable processes for advancement of high capacity batteries, tin-centered anode materials have attracted wide attention [64].

Cheol-Min Park and Ki-Joon Jeon (2011) in their experiment synthesized porous SnSb/C nanocomposites as the negative electrode for high capacity lithium-ion battery. Such porous nanocomposite materials were synthesized by a two-step process. The physical process involved high energy mechanical milling (HEMM) of SnSb/$MgCl_2$/C and in the second step was washed with

ethanol and water. The resulting product was porous nanostructured SnSb/C composite. The average particle size of the crystals was calculated to be 11 nm. This synthesis method holds several advantages over other synthetic methods. Significantly enhanced electrochemical charge/discharge profiles were observed along with large capacity and good cyclability [65].

Jian Xie et al. (2011) employed one step solvothermal route using graphene oxide, hydrated tin chloride and antimony chloride to synthesize SnSb nanocrystal/graphene hybrid composite. The authors discovered and explained that the attraction between the positively charged (Sn^{+2} and Sb^{+3}) negatively charged (graphene) layer is significant in smooth distribution of particles of the material over sheets of graphene. Compared to the bare SnSb, the nanocomposite showed increased electrochemical activity and enhanced Li-storage performance. The formation of 2D conductive networks, homogenous dispersion and confinement of SnSb particles are considered to be one of the major reason for the improved electrochemical performance. It was obvious from the results that the integration of graphene can upgrade the electrochemical properties of SnSb with prospective application as anode material for Li-ion batteries [66].

Naoki Nutta and Gleb Yushin (2013) provided a brief overview on development of high capacity anode materials over the past years. According to several research works and experiments, silicon has emerged to be a very promising candidate for anode materials for Li-ion battery systems. Other materials such as magnesium, aluminum and tin are also considered to be an interesting anode material, although they come with certain drawbacks. According to the authors, novel anode architecture might permit production of multipurpose batteries with proficiency in load-bearing, which can moreover enrich energy density. However, the main concern is the development and commercial production of high-energy and high capacity anodes for application in electric vehicles and consumer electronics. The unrelenting innovative in-situ

and ex-situ analyses, novel electrode and cell design and simulation based on theoretical models, may lead to fabrication of better performing and more feasible high capacity anodes [67]

Subrahmanyam Goriparti et al. (2014) assessed and reviewed the latest improvements in the development of active and nanostructured anode materials for next generation of Lithium-ion battery. The paper summarizes the significant role of nanoscience and technology in the improvement of anode materials. High lithium storage, lower diffusion length, and minimal anode volume change could be attained due to the exclusive physico-chemical properties of the nanostructures. Collectively, these exquisite features, can provide for high energy/power per unit volume devices. For the intercalation/ de-intercalation group it was found that while soft carbon dominates the battery industry, the use of hard carbons are an interesting alternative for increased capacity application such as efficient electricity dependent vehicles. Disregarding poor density of energy associated with titanium oxide anodes, the elevated reversible capacity, and the high power concentration make these materials excellent choice for application in high power batteries, Hybrid Electric Vehicles (HEV) and systems requiring high power. With a slight hindrance due to the production cost, graphene was also extensively reviewed for its application as anode material in battery industry. The alloying materials were studied to provide larger capacities and high energy densities. Reducing the size to nanoscale and use of conductive matrix can help reduce the extent of volume expansion as well as significant capacity loss upon cycling. The conversion materials comprising of metal oxides/ sulfides/ phosphides or nitrides are not yet commercialized because of the problems associated with them such as retention of capacity and hysteresis in the potential are overcome. Hence the review concludes that nanotechnology is the formidable methodology for the development of novel anode materials [68].

P. Nithyadharseni et al. (2015) successfully synthesized and investigated nano-sized SnSb:Co, SnSb:Fe and SnSb:Ni intermetallic alloys. Amongst the studied materials, SnSb:Co was found to exhibit highest specific capacity retention (580 mAh g^{-1}) and an efficiency approaching 98%. SnSb:Fe alloy observed a little capacity fading, while rapid capacity fading was detected in cobalt doped SnSb and nickel doped SnSb intermetallic alloys. The high capacity retention is attributed in the property of matrix elements which prevent agglomeration of metal particles as well as buffers the volume change of electrode during cycling [69].

Xiangzhong Ren et al. (2016) synthesized and examined the alloy anode composite material- $SnSnCu_x$ using reductive co-precipitation technique. Using physico-chemical techniques, determination of the morphology, crystalline structure and electrochemical studies were conducted. It was established that the presence of Copper as a dopant increased the electrical conductivity of the composite anode material. Copper also lessens the volume expansion observed by alloy anode material and impedes the cracking of SnSb alloy. Consequently, improved electrochemical results were produced. $SnSbCu_x$ recorded initial discharge capacity of 1169 mAh g^{-1} and a coulombic efficiency of 91%. After 100 cycles, the composite was able to preserve the reversible capacity of 821 mAh g^{-1} and retained 77.2% of capacity. The cyclic voltammetry and also the charge-discharge tests confirmed that the ternary composite material $SnSbCu_x$ permits a high reversible capacity and a stable cycling performance [70].

Xiaoqiu Chen et al. (2016) synthesized Sn-Sb-Co alloy particles implanted within graphene oxide via the process of co-precipitation. The processes were further followed by thermal treatments preceded by quenching of nitrogen. It was observed that the reversible capacities of these hybrid electrodes were 937 mAh g^{-1} and also possess a discharge capacity approximately equal to 734 mAh g^{-1}. The conductive graphene network credited for the excellent electrochemical

properties of the hybrid electrode material. It was discerned that the conductivity was significantly improved as a result of the volume buffering action which also prevents the aggregation of SnSb-Co particles [71].

Srijan Sengupta et al. (2017) developed Sn-Sb-Ni intermetallic alloy material infused with foam of nickel as high functioning anode material for the secondary lithium-ion batteries. The three-dimensional nickel framework improved the mechanical stability of the inter-metallic electrode material. The electrode material, which was free from any binder element, delivered a reversible capacity reaching 506 mAh g^{-1} and witnessed loss in capacity of 16% at 0.5 C. The as-synthesized hybrid electrode material exhibited better performance in the easing the volume change and possess progressive rate capability, in contrast to Sn-Sb-Ni/Ni-film [72].

Zheng Yi et al. (2017) employed one plot replacement reaction technique for fabrication of SnSb nano/micro structures. Metallic tin was used as the template as well as the reducing agent. Hollow structure was obtained when ethyl alcohol was used as the solvent and nano-sized tin as the template. The dendritic morphology was formed when micro-sized tin and ethylene glycol were used. The hollow Sn-Sb form or dendritic form, in the as anode materials for Li-ion batteries, demonstrated higher discharge capacities. "The discharge capacity of 820.7 mAh g^{-1} and a reversible capacity of 751 mAh g^{-1} after 100 cycles". The superior electrochemical performance compared to several other testified outcomes can be ascribed to "the distinct morphology and structure". Due to the structural advantage, distance of transportation of ions of lithium was reduced effectively as well as also provided additional open space which buffers the expansion in volume during the insertion and extraction of lithium. The work portrays a simplistic approach to synthesize the novel materials, with enhanced cyclic ability and good rate discharge ability. Many additional composites in the

sector of electrical devices and storage of energy urgently demand to be investigated [73].

Ali Eftekhari (2017) provided a general review about the anode material. He also emphasized on the significance of the operating voltage in context of the anode material. Pseudo capacitive behavior has been observed in substantial number of innovative anode across a varied potential gap ranging from 0 to 3.0V. This implies that the drop in the upper cutoff may significantly incur changes in the specific capacity. In the same way, a change in specific capacity can be stated for the positive electrode in case of change in the lower cutoff. The delithiation capacity is vital in anode materials as it cannot exceed the lithiation capacity. The pseudo capacitive behavior, depicted in the galvanostatic profiles shown by novel anode materials is much more distinct often represented by means of a diagonal line. Conversion reactions may occur in the anode material ensuing the growth of new materials. This might cause the de-lithiation to take a different route. As a result, it crucial to choose the lower limit of the potential window judiciously. The complexity of choice of anode materials is considerably greater than the cathode materials and is based on the potential of the electrode and the reaction mechanism [74].

Wen Qi et al. (2017) Their review encompasses the principles of processes of charge–discharge and assessment indices related to performance, the benefits and drawbacks of numerous frequently investigated materials including carbon, transition metal oxides, alloys and silicon. Several strategies and material synthesis mechanisms were examined to upgrade the performance of battery, depending upon the structural alteration of the anode material involved. Nano-structuring the materials, and development of the enhanced composites have led to considerable progress in the field of energy storage. Although, there still exist many challenges which need immediate attention. The thorough valuation of anode materials and structures is an urgent necessity, and targets to fabricate

structural designs of electrodes capable of complete better performance. Theoretical research including modelling and computing need to be employed and utilized so as to amplify the attributes which leads to enhanced performance and curtail the shortcomings amid the different materials and structures [75].

Suman Das et al. (2017) in their research work exploited the characteristic feature of decrease in volume expansion experienced by tin in the binary compound of SnSb. The main emphasis of the research was to vary the molar concentration of tin and antimony in SnSb, so as to optimize battery performance. This was carried out by varying the percentage of tin content in SnSb encapsulated within carbon nanofiber. Along with plying the electron transport route the nanofiber also contains the volume changes during charge/discharge cycles. It was found in the experimental study that the imbalance in the structure of SnSb and any loss in Sn are diminished by orderly alteration in chemical conformation of SnSb, during repetitive cycling. It was observed that the content of individual material is very critical, as the cyclability and capacity of the material are contingent on the variable content in percentage of tin. When used SnSb (75:25), which holds excess of tin, "superior specific capacity of 550 mAh g^{-1} after 100 cycles were exhibited compared to pure SnSb (1:1) anode material". The material also retains exceptional rate capability over wide-ranging current densities [76].

CHAPTER 3

EXPERIMENTAL: SYNTHESIS AND CHARACTERIZATION OF SnSb AND SnSb-ZnO

3.1. Selection of anode material

In the process of development of negative electrode materials with high energy density, life enhanced safety, low cost and long cycle, alloy anode materials are deemed important. The alloy anode materials hold certain advantage over the graphite and lithium titanium oxide anodes. These include, even at maximum volume expansion, alloy anode material exhibit 2-5 times greater charge densities in their electrochemical performance compared to graphite and LTO anodes. The moderate operating potential window of alloy anodes versus lithium is an added advantage. This potential prevents the concern regarding the safety issues associated with deposition of lithium which is very common in anodes made of graphite (~0.05V vs. Li), and also, shuns the energy loss accompanying the anode of LTO (approx. 1.5V vs. Li/Li+). Table 3.1 compares the electrochemical properties of graphite, LTO and various alloy anodes. The major drawback with alloy anodes is the the large volume change and poor cyclic stability for the duration of lithiation and delithiation processes accompanied by aggregation of particles. The limited practical application of

alloy anode is attributed in the high irreversible capacity loss during the first cycle. In order to improve the performance of the anodes several strategies are considered for synthesis and fabrication of the materials [77, 78].

Table 3.1. Comparison of electrochemical performance of alloy anodes with graphite and LTO [78]

Materials	**C**	**LTO**	**Si**	**Sn**	**Sb**
Density (gcm^{-3})	2.25	3.5	2.33	7.29	6.7
Lithiated phase	LiC_6	$Li_7Ti_5O_{12}$	$Li_{4.4}Si$	$Li_{4.4}Sn$	Li_3Sb
Theoretical specific capacity ($mAh\ g^{-1}$)	372	175	4200	994	660
Theoretical charge density ($mAh\ cm^{-3}$)	837	613	9786	7246	4422
Volume change (%)	12	1	320	260	200
Potential vs Li/Li^+ (V)	0.05	1.6	0.4	0.6	0.9

In order to prevent the unfavorable outcomes of the sizable volume change and assuage the electrolytic reactions, innovative measures have been developed and employed.

1. Multiphase Composites: The alloy particles when disposed within a matrix which serves as the host medium, helps to contain the large volume expansion and contraction experienced by the active particles. This in turn, protects the structural integrity of the electrode and maintains the electronic contact amid the conductive phase and active particles. The transport of charges is facilitated by

the host matrix, which also moderates the aggregation of active particles at the time of cycling. Depending upon the host phase, the composite can be categorized into four type viz. carbon matrix, active matrix and inactive matrix composites and also the porous structures [79].

The *inactive matrix composites* along with the active particles, also consist of chemically inert matrix such as metals (Fe, Cu), alloys (LiS_2), an oxide (Al_2O_3), or a ceramic material (TiN or SiC). When tin oxide (SnO) reacts with Li in-situ, a tin based composite oxide anode is formed as a result of Sn nanocrystals being dispersed in the mixed oxide matrix [80]. "The cycling stability of composite anodes is excellent (over 100 cycles) at a reversible capacity of 600 mAh g^{-1} which is on account of higher amount of host phases". SEM examinations of Al/SiC composites witnessed no cracking during first cycling unlike pure aluminum (Al) anode. This occurs as a result of buffering action of the matrix. Although, the drawback of such a matrix is slow lithium and electron transport which eventually results in low capacity. To overcome such a problem, a matrix with low ductility, low elastic modulus, and enhanced strength as well as with good ionic and electronic conductivity must be chosen [81].

In the anodes developed from *active matrix composite,* the active phase together with the host medium, is involved in the process of lithiation. In the process, when one component undergoes lithiation, the other acts as a buffer which alleviates any change in the volume. This happens on the account of different onset potentials for reaction with lithium (Li). Considering, our choice of material as a specimen, which is tin-antimonide, antimony (Sb) being the more reactive phase, reacts with lithium at ~0.9V vs. Li/Li^+ while tin having an onset potential around ~0.6V helps in the containment of the drastic increase in the volume of the lithiated phase of antimony. The depth of charge of such type of composites modulate the cycling stability. Consequently, a better cycling stability can be achieved by limiting state of second component lithium insertion [82].

Carbon matrix composites are considered as a favorable choice due to the superior electronic conductivity and buffering effect of carbon. Presence of carbon as an additive also provide the advantages of good ionic conductivity, low volume expansion, and lithium-storage ability. Existence of coating of carbon on silicon not only suppresses the formation of SEI layers but also opposes the volume expansion during lithiation. In addition to particle size control and better capacity retention, carbon composites also provide high cyclic stability [83].

Porous electrode structures having a three-dimensional structure can easily accommodate large variation of volume at the expense of their porosity. The fabrication involves depositing the material using electricity over a current collector, which is porous in nature or even over a template. However, the total volumetric density of the cell is diminished due to the presence of considerable volume of pores. Therefore, this calls for an urgent need for increase in the practical loading of active material.

2. *Control of particle size:* Many studies have reported that once the size of active material is reduced to nano dimension, there is a significant improvement in the cyclic performance of alloy anodes, which is most evident in the composite matrix anodes. Decreasing the size of Sn to 300 nm indicate significant increase in total stable cycles. The increase in the cyclic stability results from the increase in the yields and fracture strengths of the active materials, due to decrease in grain size to nanometer scale. The average diffusion length is also decreased due to reduction in the particle size, which enhances the electronic and ionic transport and additional Li storage sites. However, size reduction to nanometer range also results in self-discharge and poor cycle life, occurring as a consequence of increase in side reaction and SEI formation [84].

3. *Intermetallics:* As previously discussed in intermetallic anodes a lithium insertion host structure is created which supports the structural integrity between parent, intermediate, and the lithiated products, thereby preventing the volume expansion. The intermetallics contain stable sublattice, although the host lattice undergoes lithium insertion by simultaneous extrusion of the second component. The widely studied intermetallics include Cu_6Sn_5, InSb and Cu_2Sb. Intermetallics also exhibit stable cycling performance over number of cycles which is accredited to the structural stability, fast chemical kinetics and restricted volume change provided by the insertion of the lithium and extrusion of metal [85].

4. *Thin film and amorphous alloys:* Anodes which are fine and delicate have gained wide attention ever since the excellent cycling performance and stable capacity retention ("2000 mAh g^{-1} /1000 cycles") of the thin layer of silicon anodes were reported. Such desired properties were ascribed in the robust adherence of the active material to the conductive layer. There are several causes for the functioning of the anodes fabricated in the form of thin films, the most important of which are temperature, substrate-surface roughness, deposition rate and thickness of the films. It was observed that the cycle life reduces with the increase in the thickness of the film, while experimenting with deposition of thin Si film on a nickel foil. This ensued from the increase in the lithium diffusion length, larger stress, and higher internal resistance while lithiation and delithiation. The drawbacks include expensive deposition and low rate of loading of active material [86].

5. *Operating voltage:* It has been reported, that cycling within a limited range of voltage, resulted in better cycle life. Limiting the upper or lower cutoff voltage, helps in preventing excessive volume change, particle aggregation and structural change. Experimentally it was noticed that slight increase in the lower cutoff potential from 0V to 0.8V, Sb/C nanocomposites exhibited better cyclic performance. Likewise, the amorphous silicon samples were detected with

increased cycle life from 40 to 200, whilst change in the lower cutoff voltage was from 0V to 0.2V. Also, amorphous Si showed better capacity retention as the upper limiting voltage was decreased to 0.8V from 2V. However, voltage control provides these advantages at the cost of anode capacity [87, 88].

Apart from the above strategies, the choice of binder system and appropriate electrolyte are essential for productive and profitable commercialization of alloy anode materials. Keeping in mind all the above strategies to fabricate efficient alloy anode material, tin-antimonide (SnSb) active matrix nanocomposite material was selected for the experimental project. A brief discussion on the process of synthesis, effect of dopant material, physical characterization and electrochemical studies is discussed henceforth [89].

3.2. Synthesis of materials

All the materials used in the synthesis of the nanocomposite are of analytical quality. Four different samples were synthesized. SnSb-$(ZnO)_x$ active phase alloy composites were synthesized in the molar ratio 1: 1: x, (x = 0, 0.08, 0.2 and 1.2). In a typical experiment, 0.03 M of Sn (99.9%), Sb_2O_3 (99%), and ZnO were mixed together and subjected to high energy ball milling for 18 hours. Small quantity of ethanol was added to the ball mill cylinder which prevents corrosion and ease up the mixing of the materials. The mixture of reduced particles was then moved to an autoclave made of stainless steel and maintained at 160°C for 12 hours under vacuum. The final products were then isolated and stored under inert atmosphere. The overall synthetic procedure is schematically depicted in the Fig 3.1. Proper precautions and care were taken to prevent the contamination of the samples from any kind of impurities. All the apparatus and equipment used were thoroughly cleaned and sanitized prior to the synthesis process. The materials used were laboratory grade and free from the presence of any impurity.

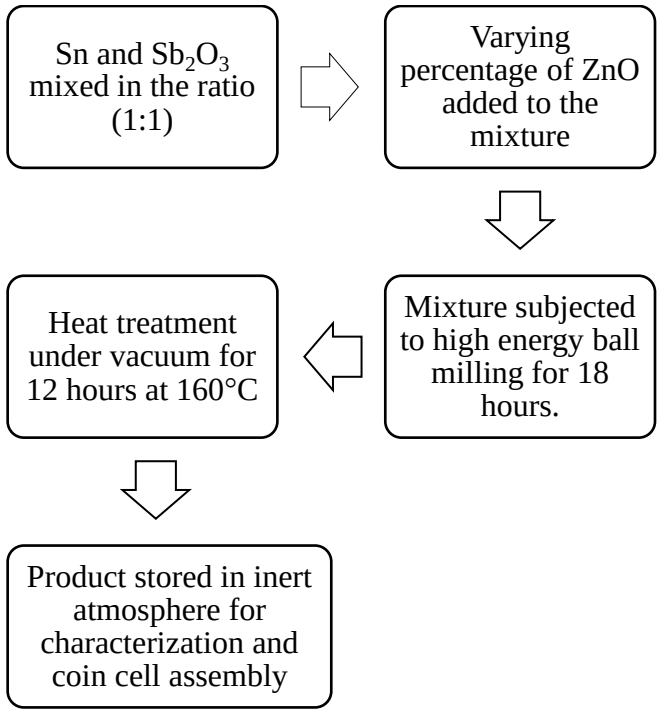

Figure 3. 1. Stepwise diagram for synthesis of nano-sized ternary SnSb-ZnO composite

3.3. Physical Characterization

3.3.1 X-ray Diffraction

The phase identification of a crystalline material is carried out using "X-ray powder diffraction (XRD)". X-ray diffraction is an analytical procedure which provides information about the dimensions unit cell. X-ray diffraction found its origin in von Laue's experimental discovery in 1912 in which he postulated that crystal diffract x-rays. In his hypothesis Laue explained that materials which are crystalline in nature behave as 3-dimensional diffraction gratings for the X-rays with wavelength analogous to the plane spacing in a crystal lattice. The pattern of diffraction reveals the crystal structure of the material. This technique is also used for analysis of chemical composition, measurement of stress, particle size measurement, single crystal orientation as well as the orientation in a polycrystalline material. Bragg's Law is the basis of understanding of X-ray diffraction. That is to say that the monochromatic X-rays undergo diffraction

only when the angles of incidence satisfy the Bragg's law. "X-ray diffraction is based on constructive interference of monochromatic X-rays and a crystalline sample" [90]. Consider a section of a crystalline material, with atoms arranged on the parallel planes, d distance apart, as we can see in the Fig 3.2.

Suppose a paralleled beam of monochromatic X-rays with wavelength λ are being incident at the crystal structure an angle of θ, known as the "Bragg's angle". This is the angle between the incident ray and the plane of incidence. Ray 1 is reflected off the first atomic plane, while Ray 2, travels a little deeper to the second atomic plane, and reflects off. In doing so the second ray 2-2′ travels a distance DE + EF greater than the 1-1′. Therefore, we can say, that the path difference DE + EF = 2d sin θ. According to Bragg's law, "diffraction (constructive interference) occurs only when the wavelength of the wave motion is of the same order of magnitude as the repeated distance between scattering centers". Hence, we can write,

$$2d \sin \theta = n\lambda$$

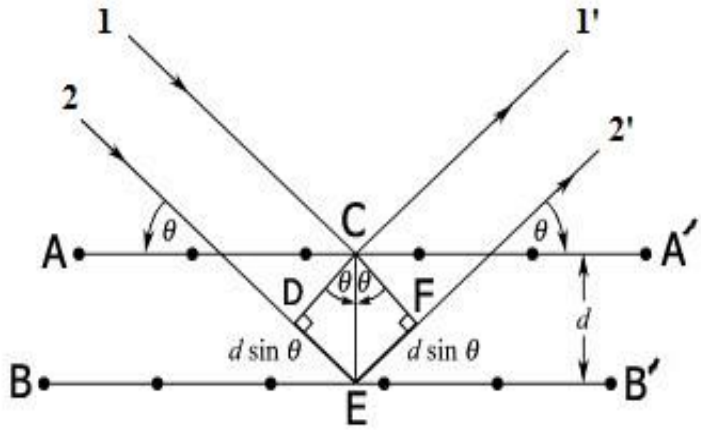

Figure 3. 2. X-ray diffraction and Bragg's Law

We can say, in an X-ray diffraction experiment we observe a set of intensities and the angles at which they are diffracted. The observed diffracted X-rays can

be identified, treated and tallied. Due to random orientation of atoms within a powdered sample, so as to obtain all the probable set of lattice direction, the sample is scanned for a varying range of angles of 2θ. The material identification is done by converting the diffraction peaks to d-spacing. These spacing are verified by comparison with the benchmarked reference patterns [91].

The three main components of an X-ray diffractometer are: “an X-ray tube”, “a sample holder”, and “an X-ray detector”. In a cathode ray tubes the filament is heated which produces electrons. By applying a voltage these electrons are fast-tracked towards a target. This voltage is applied by means accelerating plates. These hastened electrons bombard the target. The electrons containing sufficient amount of energy when hit the target material, it removes an electron from the inner shell, thereby producing the “characteristic X-ray spectra”.

The X-ray spectra consists of various components, K-α and K-β. Kα has two components, $K\alpha_1$ and $K\alpha_2$, with former having twice the intensity of $K\alpha_2$ and a shorter wavelength. “The most common target for single crystal diffraction is copper with CuKα = 1.5418 Å”. These X-rays are then collimated and guided towards the rotating sample and detector, where the intensity of each reflected X-ray is recorded. A peak in the intensity is observed when the incident X-ray on the sample satisfies the Bragg’s equation. These intensities are recorded and converted into a count rate, which forms the output. In a diffractometer the sample rotates at angle θ, and receives the collimated X-rays. The diffracted X-rays are received by a detector which is mounted on an arm and rotates at angle 2θ. The device which rotates the sample and helps to maintain the bragg angle is known as goniometer. In general, data is collected in the values of θ varying from ~ 5° - 70°. Apart from determining the crystal structure and phase analysis, “X-ray diffraction can also be used to characterize thin film samples in order to determine lattice mismatch between film and substrate, dislocation densities, orientation of grains and sample purity” [92].

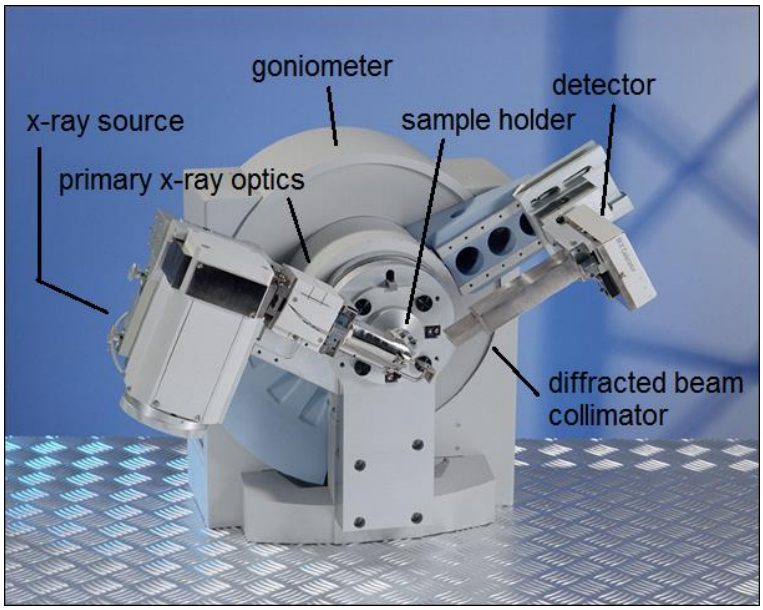

Figure 3. 3. X-ray diffraction machine

The as-prepared sample were characterized using "X-ray diffraction (XRD, PANalytical X'pert PRO)" using CuKα radiation (CuKα = 1.5406Å) with θ varying in the span of 10°-70° to determine the structure of the crystal and the phase analysis.

3.3.2 Scanning Electron Microscopy

In a scanning electron microscope, a stream of high energy electrons are used to produce signals at solid surface of the material under study. The signals which are obtained by the interaction of electrons with the sample surface provide a variety of information such as surface topography, chemical composition, crystallinity, and material orientation. The data of a specific area is collected and an image is generated revealing the spatial variation in properties. A conventional SEM in scanning mode can image areas ranging from 1 centimeters to 5 micrometers, providing magnification varying from 50 X to 10000X and a spatial resolution in the range 10 to 100 nm. In order to produce an image, the

detected signal is combined with the position of the electron beam, which is scanned in a “raster scan mode” [93].

The electrons emitted from a thermionic source or a “field emission source” and are accelerated in a high gradient of electric field. These primary or major electrons are focused by a pair of condenser lenses and deflector plates such that they are deflected in a manner to produce a raster scan of the surface of the sample. When these electrons bombard the sample, the high kinetic energy of the accelerated electrons is dissipated by repeated random scattering and absorption in the production of various signals during the electron-sample interaction. The signal resulting from the energy exchange includes secondary electrons which form SEM (topographical) images, backscattered electrons which provide information on contrast between areas with different chemical composition, diffracted backscattered electrons(EBSD) which helps in determination of crystal structure and mineral orientation, characteristic X-rays which can be used for elemental mapping (EDX), continuum X-rays, visible light, auger electrons which help in determination of surface atomic composition and heat [94].

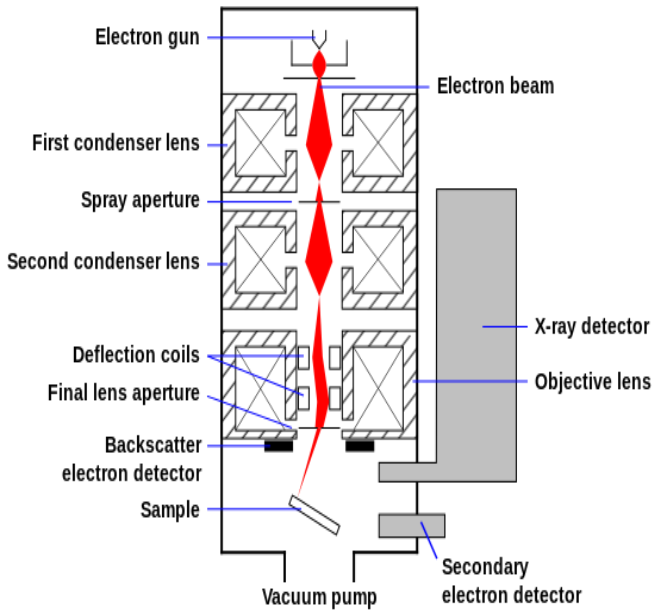

Figure 3. 4. Illustration of working of SEM

High resolution images of shapes of the samples are produced using SEM. It also helps in elemental mapping and chemical analyses using EDX/EDS, phase distinction in multiphase specimens with the help of back scattered electrons (BSE). The production of (cathodoluminescence—CL helps in compositional mapping. In addition, SEM also helps to distinguish different phases depending on qualitative chemical examination or the crystal structure. Accurate measurement regarding determination of very minute features and objects as small as 50 nm in size. Modern day SEM generate highly portable data in the form of digital images. The majority of SEMs use a "solid state x-ray detector (EDS)". Even though such SEM's are easy to utilize and fast, they still suffer from relatively poor resolution of energy and are sensitive to elements present scarcely. Electrically insulating samples need a conductive coating for analysis in typical SEM [95].

Figure 3. 5. A typical SEM instrument

The samples were also examined using "Scanning Electron Microscopy (SEM, ZEISS ULTRA 55)" so as to determine the external surface morphology of the particles. Thermogravimetric analysis (TGA was carried out from room temperature to 1000°C with the heating rate of 10°C min $^{-1}$ in air.

3.4. Electrochemical Measurement

For the electrochemical study, the equipment used was Mbraun make glove box 106 having O_2 and H_2O level ≤ 0.5 ppm. To assess the electrochemical properties, the electrodes were fabricated by mixing 80 wt% of main material, 5 wt% of carbon black (or acetylene black) and 15 wt% of a binder known as polyvinylidene fluoride (PVDF) to form a mixture. The resulting slurry was spread evenly over a thin foil of copper. Copper is used as a substrate because it plays the role of the current collector for negative electrodes of a Li-ion battery. The spread coating was dried at 120°C for a time period of 12 hours under vacuum. The metal foil, dried and coated, was pressed via calendaring. The pressed foil was then punched into numerous small discs, measuring 8 mm in diameter. The electrode was weighed and transferred into the glove box for fabrication of coin cells.

Assembly of "Coin cells (CR2032) was performed in an argon filled glove box" for measurement of electrochemical performances. In the coin cells, the role of counter electrode is played by metallic lithium foil. The electrolyte used was a solution of 1 M "$LiPF_6$" mixed in "ethylene carbonate (EC)–dimethyl carbonate (DMC) (1:1)". Coin cell cases, separators (CELGARD-2400), springs and spacers were transferred into the glove box. In order to assemble the coin cell, electrolyte was filled, after the proper placing of the working electrode (SnSb and SnSb-ZnO), strips of counter electrode (Lithium metal) and stainless-steel separators. Finally, the cell was closed using the cap casing of the cell and was crimped using the crimping machine. Any excess electrolyte is cleaned. The cell was then taken out of the glove box for tests which include, Cyclic Voltammetry (CV), Electrochemical Impedance Spectroscopy and Galvanostatic charge-discharge (GCD). Cyclic voltammetry experiments were conducted over a potential window varying from 0.1V to 3.0V vs. Li/Li^+. "Electrochemical Impedance Spectroscopy (EIS)" was conducted using an AC voltage pulse of 5 mV. The frequency range of the AC pulse was set between 10

kHz-10 mHz. All the electrochemical tests were performed using “EC LAB cell test system” at room temperature (i.e. ~300 K.)

CHAPTER 4

RESULTS AND DISCUSSION

4.1. Analysis of XRD data

Fig 4.1 shows the X-ray diffraction patterns of SnSb-ZnO nano-composite material with varying compositionS of ZnO, synthesized via mechano-chemical activation technique. For bare SnSb sample, apart from a few minor peaks of Sn, no impurity peaks were observed in the diffraction pattern. The observed peaks for bare SnSb correspond to the rhombohedral structure of β-SnSb phase which belongs to the space group $R\bar{3}m$. In the diffraction pattern of SnSb-ZnO composite, the sharp peaks of SnSb, Sn and ZnO are distinctively observed along with a few weak peaks of SnO_x, SbO_x, and Sb. It can be established from the diffraction patterns, that a slight increase in the ZnO content, there is gradual decline in the peaks of SnSb and Sn. The incorporation of ZnO in the SnSb alloy composite, results in samples with two intermetallic phases, comprising of β-SnSb phase and hexagonal ZnO phase. A few minor impurity peaks were noticed. The average crystallite size for the SnSb and SnSb-ZnO alloys based on the main peak (101) was calculated to be in the range 21.7 – 25.5 nm. This was calculated using the Debye-Scherrer formula, which indicated that the crystallite size increases, when bare SnSb is coated with the ZnO.

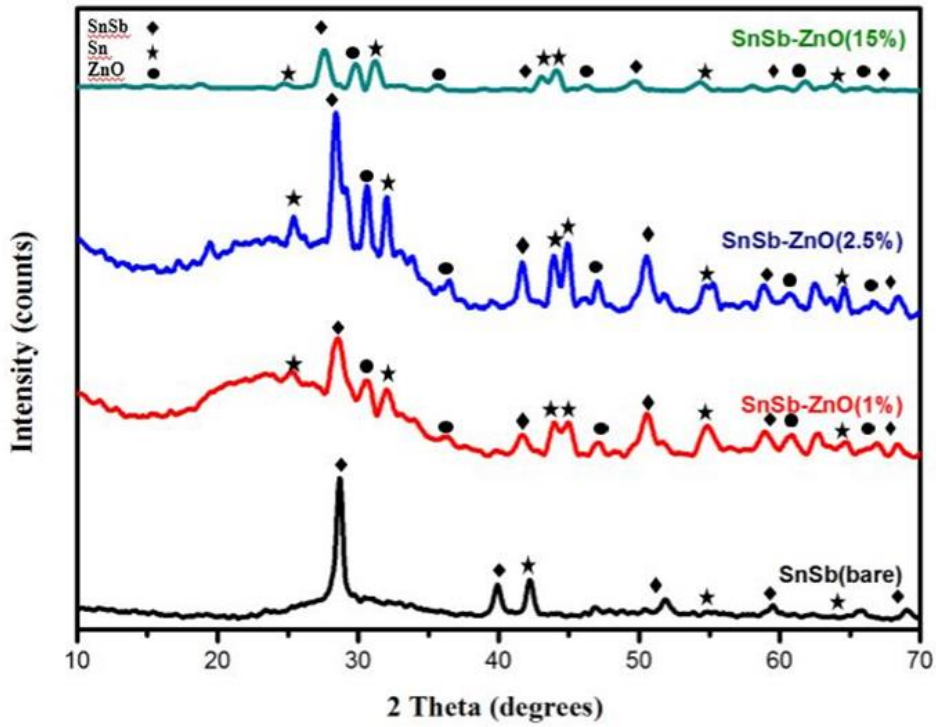

Figure 4. 1. Pattern obtained by X-ray diffraction analysis of bare SnSb and SnSb-ZnO (1%), SnSb-ZnO (2.5%), and and SnSb-ZnO (15%) composite.

4.2. Analysis of SEM and EDX data

In the Fig. 4.2 (a-d) can be seen the SEM images of SnSb and SnSb-ZnO nanocomposite. The results indicate very small particles of SnSb and SnSb-ZnO. The average grain size observed were 2.5 µm. The obtained images show homogenous distribution of tiny irregular particles which also seem to have undergone uniform aggregation. The particle size was observed to increase with increase in the ZnO content in the sample.

The elemental analysis of each sample, in order to verify each component present in the sample along with their relative abundance was detected using EDS microanalysis as shown in Fig 4.3. From the EDS microanalysis results, the presence of each elemental component i.e. Sn, Sb in bare SnSb sample and

Sn, Sb, Zn, and O in SnSb-ZnO samples was verified. From the quantitative analysis of each sample, the weight percentage and atomic percentage of individual component were revealed. Bare SnSb has 43.35% Sn, 46.66% Sb, and 7.11% O content. Similarly, SnSb-$ZnO_{0.08}$ has 33.92% Sn, 36.01% Sb, 0.69% Zn, and 29.38% O content. SnSb-$ZnO_{0.2}$ has 35.68% Sn, 33.12% Sb, 1.01% Zn, and 30.18% O content. SnSb-$ZnO_{1.2}$ was observed to contain 39.20% Sn, 32.54% Sb, 2.10% Zn, and 26.16% O content.

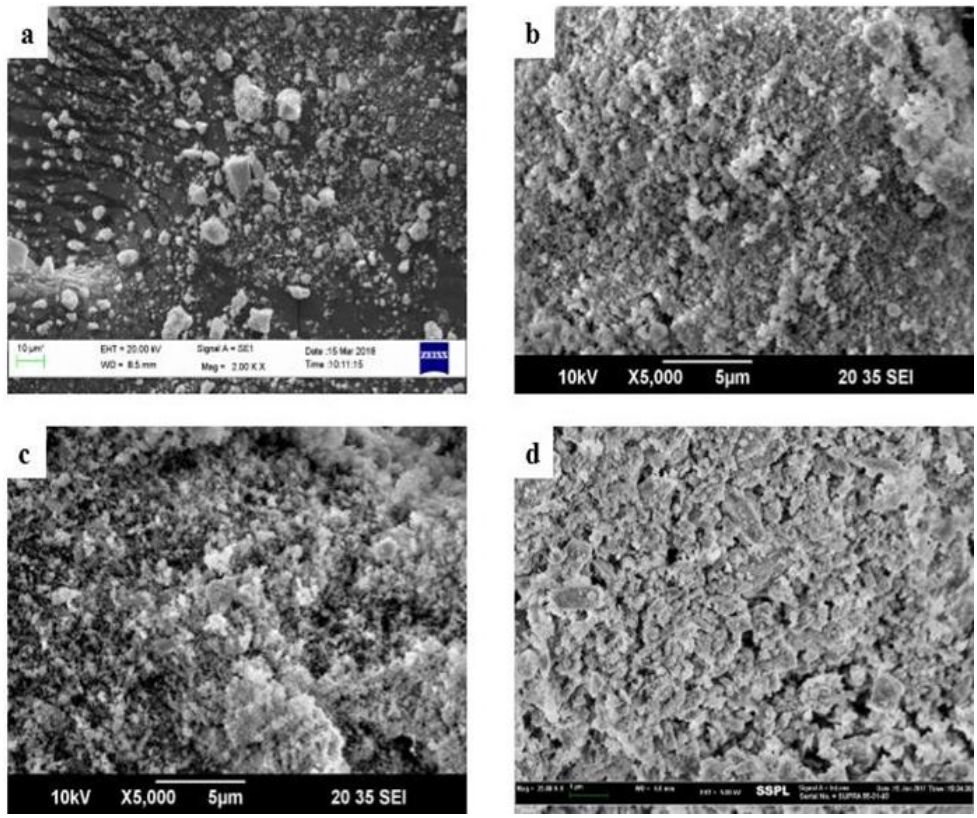

Figure 4. 2. SEM images of (a) bare SnSb, (b) SnSb-ZnO (wt 1%), (c) SnSb-ZnO (wt 2.5%) and (d) SnSb-ZnO (wt 15%)

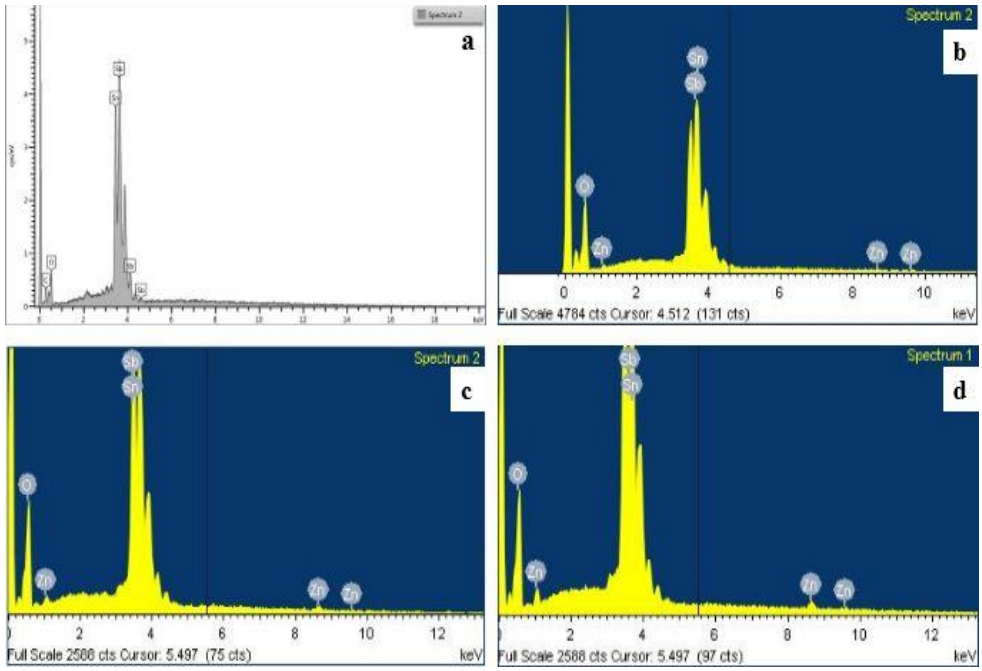

Figure 4. 3. EDS microanalysis of (a) bare SnSb, (b) SnSb-ZnO (wt 1%), (c) SnSb-ZnO (wt 2.5%) and (d) SnSb-ZnO (wt 15%)

4.3. Electrochemical performance of SnSb-ZnO_x composite

7.3.1. CV Analysis

Fig. 4.4 (a-c) show the CV plots of bare SnSb and SnSb-ZnO nano-composite materials with scan carried out at the rate 0.05 $mVsec^{-1}$ over a voltage scope between 0.01-3.5V vs. Li/Li^+. It is evident from the plot that over the given potential window, the synthesized samples exhibit only the characteristic redox peaks of SnSb. In the first cathodic scan, a broad reduction peak can be observed at around 1.3-1.5V, which is seen to disappear in subsequent cycles. The peak could be attributed to the disintegration of the electrolyte and formation of layer of SEI (solid electrolyte interface). A significant discharge (reduction) peak is observed approximately around 0.75V which is persistent in following cycles. This peak can be attributed to the lithiation reaction resulting in the formation of Li_3Sb and release of metallic tin. The broad reduction peak around 0.35-0.4V correspond to the alloying reaction between Sn and Li, resulting in the formation of Li_xSn. The peaks appearing after 0.66V conform to the reaction of ZnO with

Li which are very obscure. During the anodic scan, the de-lithiation of Li_xSn during the first cycle, can be ascribed to the oxidation peaks close to 0.6V. Similarly, the presence of an oxidation peak around 1.1V is accredited in the de-alloying process leading to conversion of Li_3Sb to Sb and resulting in the formation of SnSb alloy. The good electrochemical reversibility is implied by the presence of stable and reversible peaks in second and third cycles. The difference in the CV plot for SnSb and SnSb-ZnO composite result from the involvement of ZnO in the intercalation reaction.The overall reactions involving lithiation and de-lithiation of bare SnSb and SnSb-ZnO composite are as follows.

$$3Li + SnSb \rightleftharpoons Li_3Sb + Sn$$

$$xLi + Sn \leftrightharpoons Li_xSn \ (x \leq 4.4)$$

$$2Li + ZnO \rightleftharpoons Zn + Li_2O$$

$$Zn + xLi \rightleftharpoons Li_xZn$$

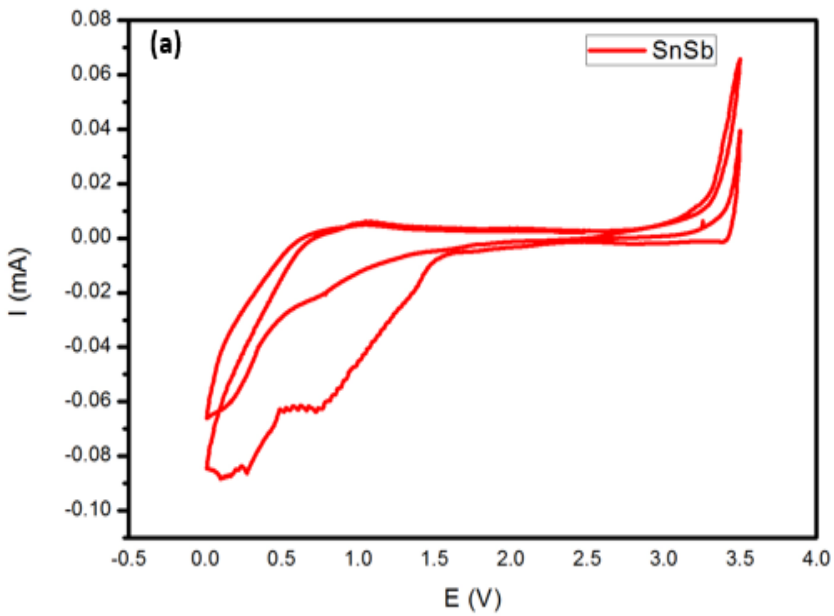

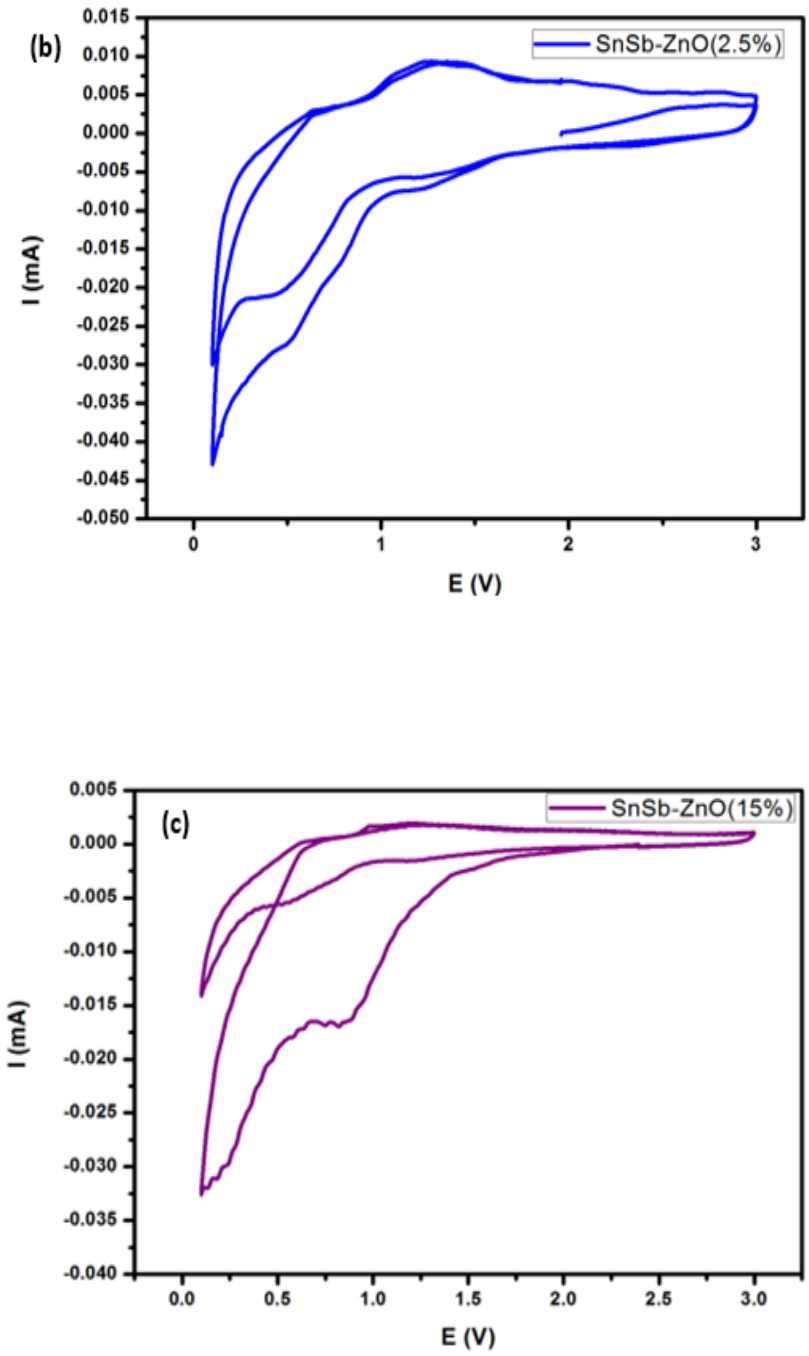

Figure 4. 4. CV curves of (a) SnSb(bare), (b) SnSb-ZnO (2.5%) and SnSb-ZnO (15%) composites

In order to better explain the electrochemical behavior of the bare SnSb and SnSb-ZnO, the ac impedance plots were recorded before cycling. EIS was conducted in the scanning frequency range of 10 mHz to 10 kHz at ac voltage amplitude of 5 mV.

4.3.2. EIS Analysis

The impedance spectra is observed to form a dampened arc or semi-circle in the region spanning from high to medium frequency and a sloping linear graph in the region of low frequency of "nyquist plot". The nyquist plots thus obtained are fitted by the equivalent circuit in the insets of the Fig. 4.5. The intercept of the semi-circular arc on the Z′ axis present in high frequency region corresponds to the electrolyte resistance, and is denoted by R_s in the equivalent circuit. The semi-circle prominent in middle frequency section represents charge transfer resistance (R_{ct}) corresponding to several reactions occurring at the electrode/electrolyte interface. CPE represents the constant phase angle elements which is associated with the double layer capacitance. W_s refers to the Warburg resistance, and it represented by the inclined line present across the low frequency zone. It is related to the Li-ion bulk diffusion resistance. The increase in the ZnO percentage leads to the increase in the radius of the semi-circle. However, the intercept observed in the region of high frequency and the linear component does not vary much with the ZnO content. The results of fitting of R_s and R_{ct} are summed up in the table 4.1. From the data of EIS, it seems that sample SnSb-ZnO (2.5%) has least impedances over all amongst all four compositions of bare SnSb, SnSb-ZnO (1%), and SnSb-ZnO (15%). Hence, the electronic and ionic conductivities of SnSb-ZnO (2.5%) may be better. Hence the composition of SnSb-ZnO (2.5%) would be prospective of good anode material for Lithium-ion battries.

Table 4.1. Impedance parameters of SnSb-ZnO nano-composies

Impedance	SnSb	SnSb-ZnO(2.5%)	SnSb-ZnO(15%)
R_s	73.48	6.507	33.57
R_{ct}	748.9	242.2	770.5

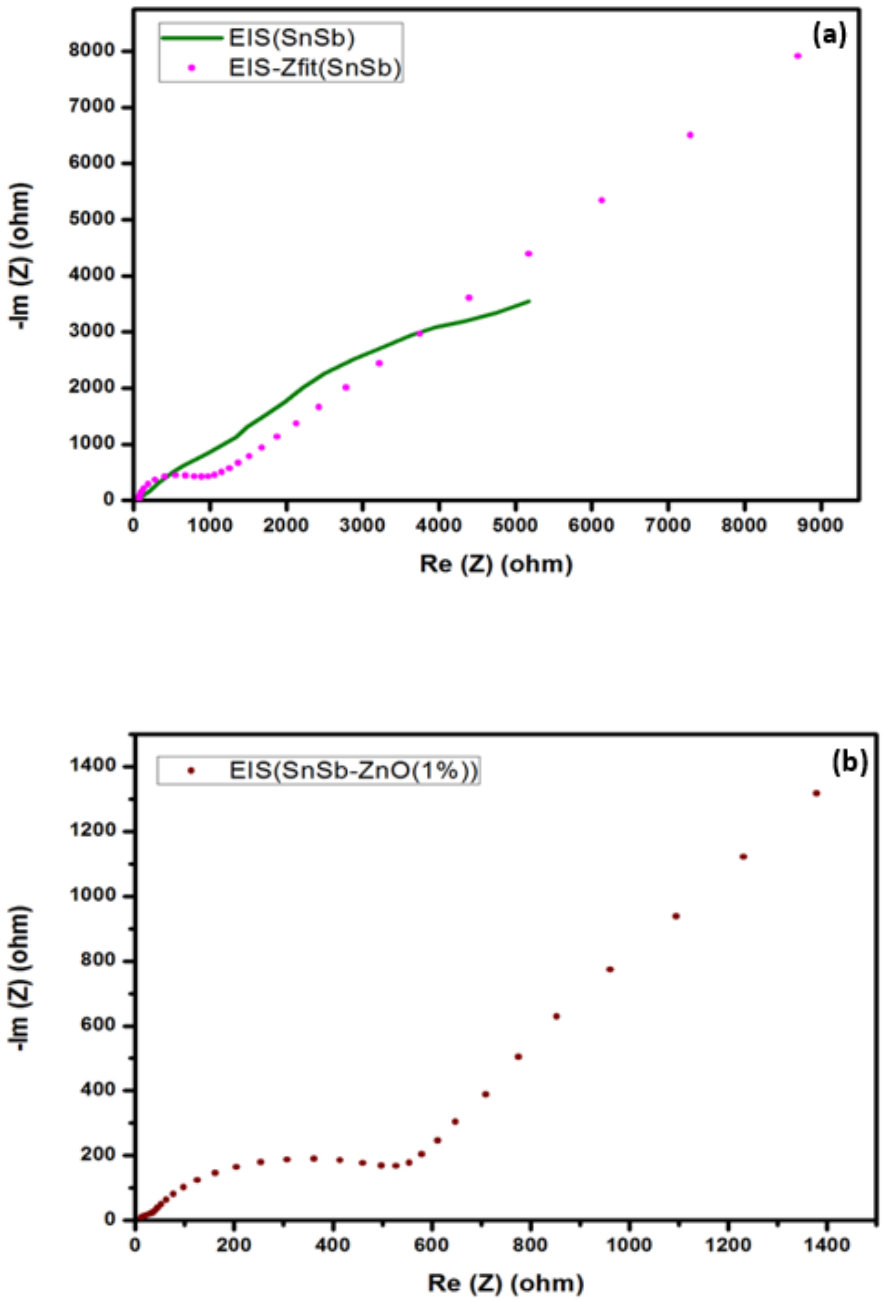

Figure 4. 5. EIS of (a) bare SnSb and (b) SnSb-ZnO(1%)

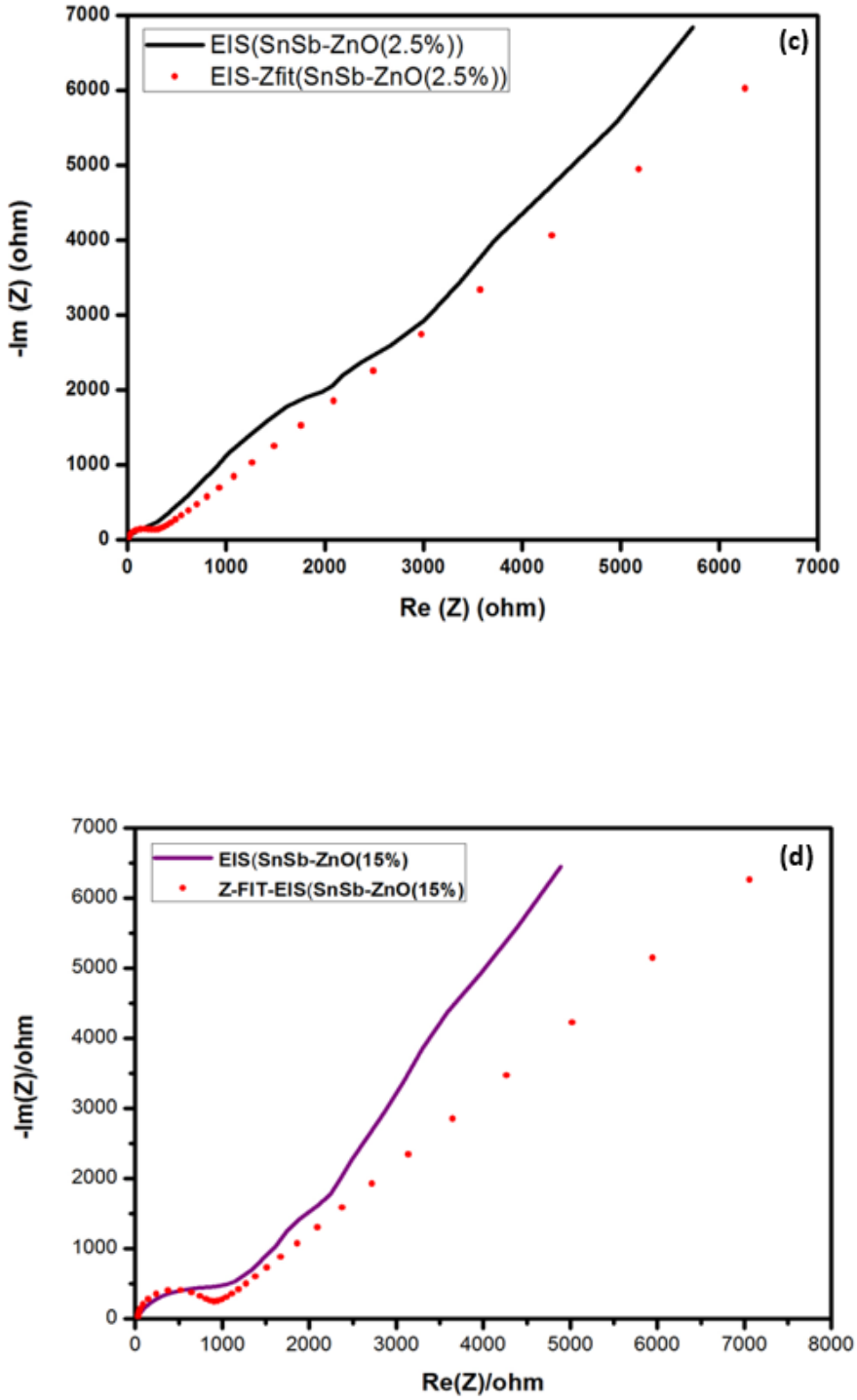

Figure 4. 6. EIS of (c) SnSb-ZnO(2.5%) and (d) SnSb-ZnO(15%)

CHAPTER 5

THEORETICAL SIMULATION OF SnSb FOR ELECTROCHEMICAL PERFORMANCE

5.1. Introduction

In this study, we have developed a simulated model by taking inputs from the 2D Lithium- ion Battery model available in COMSOL multi-physics. The use of simulation for the study the lithium insertion and extraction and charge-discharge behavior of Lithium-ion battery for a given set of material properties. The cell geometry is a two-dimensional model set up. The present investigation targets to elucidate that the several complicated issues which are linked with the study and development of anode materials. In the study for half-cells, material for anode is customarily examined as a cathode with regard to a metal foil of lithium anode. This is true for both conventional coin-type cell and also for the mathematical model. The processes of charge and mass transport in solid and solution phase included in the model constitute the electronic conduction and charge transport of ions in the electrodes and also in the electrolyte, kinetics of Butler-Volmer electrode employing the use of practically measured discharge curves intended for potential achieved at the time of equilibrium, and material transport within the spherical particles. The model developed for this study has

a half cell coin cell consisting SnSb as a porous electrode with a polymer electrolyte of $LiPF_6$ in 1:2 EC: DMC ratio.

5.2. Model Definition and Parameters

The three-dimensional (3-D) cell geometry can be seen in the Fig 5.1. Using the 2-D cross section, the 3-D geometry can be modeled as a result of along the height of the battery. Fig 5.1 shows the positioning of the positive electrode, the negative electrode, and the current accumulator which is fastened with the positive electrode. The positive electrode is porous and the negative electrode consists of lithium metal. Due to the fact that the electrochemical reactions occur only at the surface of the lithium metal and high electronic conductivity, the thickness can be neglected in the model geometry. During discharge, the porous electrode acts as the cathode and the contact of the metallic tab acts as a current collector. The negative lithium metal electrode acts as the anode and current feeder. The current and material balances in the lithium-ion battery are defined and solved using the model. A fourth independent variable for the particle radius is used to solve the insertion of lithium inside the particles in the positive electrode. The parameters used in the making of the model are listed below. The input values in the model were taken from the global parameter list as well as the material list of the model [96]. Some parameters were also calculated using the experimental data. The physical parameter of the coin cell such as the dimension of the electrodes, separator, and volume fraction were provided as an input in the model along with the electrode current.

Table 5.1. Porous electrode material content parameters

Name	Value	Description
Sigma	65 S/m	Electrical Conductivity
D	1 e-14	Diffusion Coefficient
k	28 W/m-k	Thermal Conductivity
cEqref	278000	Reference Concentration

The electrolyte used to build the model is unvaried and exactly the same that was used to build the fabricated cells. The material parameters related to the LiPF6 in 1:2 EC: DMC were used as input into the model in COMSOL. These parameters are defined in the Table 5.2.

Table 5.2. Electrolyte material content parameters

Name	Value	Description
transpNum	0.363	Transport Number
fcl	0	Activity Dependence
D	$7.5e^{-11}$ m^2/s	Diffusion Coefficient

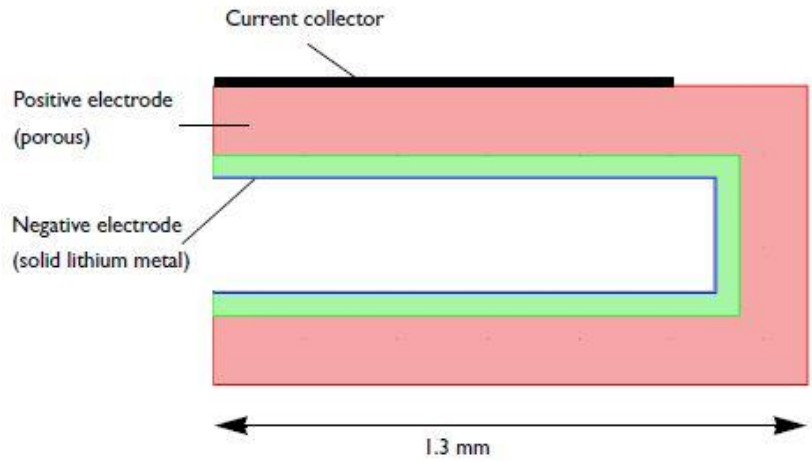

Figure 5. 1. A 2-D cross-sectional model geometry

The distribution of the depth of discharge in the porous electrode, as a function of discharge time, is shown with the help of 2D simulation. The positioning of the thickness of the porous electrode and collector of current as well as the electrolyte along with electrode kinetics and the transport properties is determines the distribution of the depth of the discharge.

Domain 1 is the porous electrode and is associated with the SnSb material. The properties of both the electrolyte and electrode are defined to characterize porous electrode. Domain 2 is associated with the electrolyte $LiPF_6$ in 1:2 EC: DMC. Under the volume fractions section, in the ε_l text field, the input value was entered as 1-0.4-0.172. The electrolyte conductivity under the effective transport parameter correction section was changed to the Bruggeman. Similarly, the electrical conductivity and diffusion were also set as Bruggeman. The boundary 10 was selected for the current collector and the electrode current density was input from the experiment data. The lithium foil negative electrode was defined by the boundaries 5, 7 and 12. Time dependent solution was set for 2700 seconds. The solution was stored at a 10 second interval during the first 100 seconds and at 100 seconds interval during the last 2600 seconds [97].

5.3. Observations and Results

The simulation shows the distribution of the concentration of lithium on the surface the electrode particles by the end of 2700 secs. The initial lithium concentration in the porous electrode is 1000 mol/m^3. Throughout the discharge process, as lithium is dissolved on the negative lithium metal electrode, the lithium concentration in the porous electrode increases.

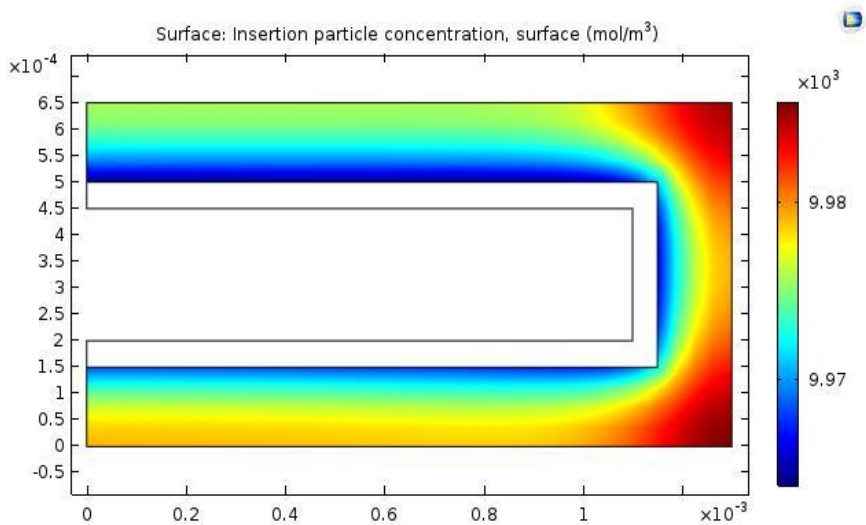

Figure 5. 2. Concentration of lithium at the surface of electrode particles

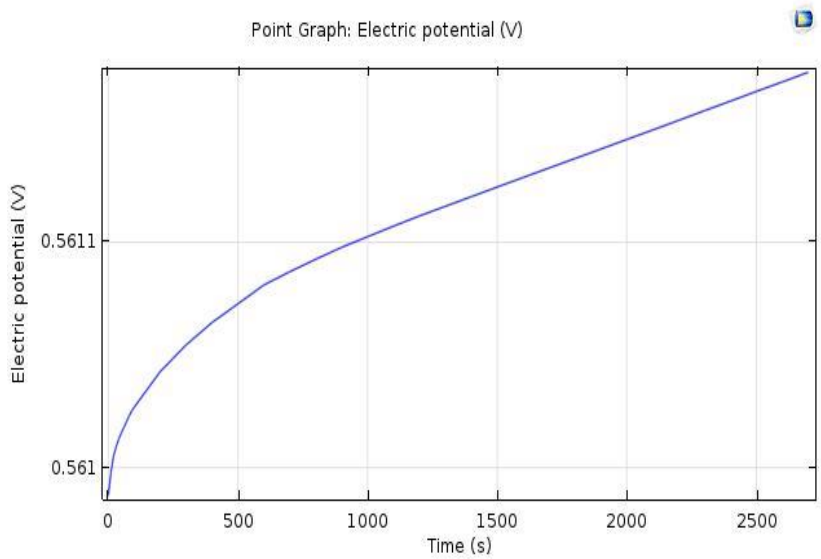

Figure 5. 3. The time-dependent cell voltage predicted by the model during the discharge simulation

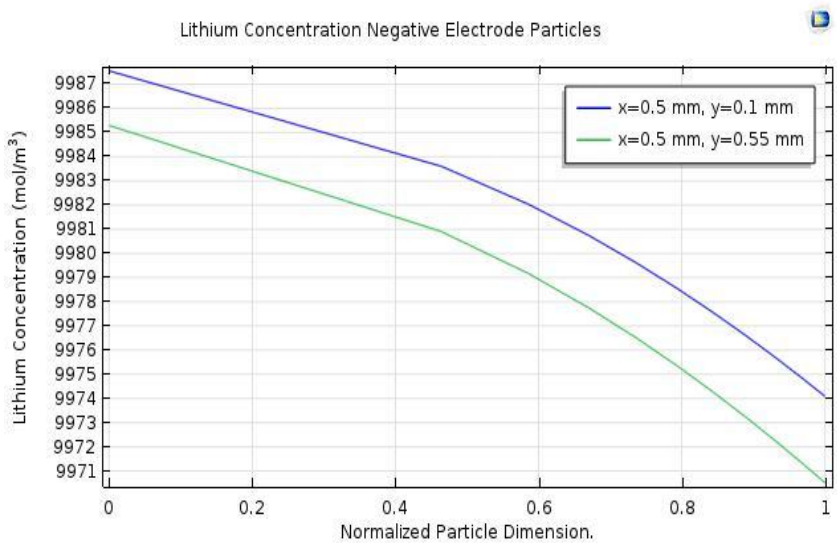

Figure 5. 4. Lithium concentration in the electrode particles at two selected positions, within the model geometry

Fig. 5.3 shows the cell voltage of the model during the simulation. The concentration in the positive electrode particles at two selected locations within the porous electrode is displayed in Fig 5.4. The green line displays the

concentration at the location furthest away from the current collector and shows that less discharge has taken place there (concentration lower).

CHAPTER 6

SUMMARY AND CONCLUSION

The project work encompasses the need of development of renewable sources of energy, advancement of Lithium-ion technology and its importance in the field of energy storage. The thesis extensively describes the strategies for selection of suitable anode material, procedure for fabrication of lithium-ion coin batteries, the physico-chemical analysis of the materials associated, and a brief comparison of experimental and theoretical/stimulated data. However, the mathematical/theoretical work is still under study, for development of models with different materials and deeper analysis of the simulation results.

It is well established that the criteria for selection and development of practical anode materials is low potential, specific capacity and cyclability. Keeping this in mind, SnSb based anode materials were focused. A ternary SnSb-ZnO_x active matrix nano-composite were synthesized via physical route (high energy ball milling). Hence, the developed anode material, based on SnSb-ZnO (2.5%) lead to better battery performance with low potential window. In conclusion, the presence of ZnO resulted in decrease in the agglomeration of SnSb alloy. This resulted in significant decrease in the lithium ion diffusion distance, lithium-insertion in the active materials was reduced, and the space available for volume expansions increased. As a result, improved cyclability is observed. The CV curves verify the multistep lithiation and de-lithiation occurring in the composite. The electrochemical performance establishes the

nano-composite as an important anode material owing to formation of stable “solid electrolyte interface film” as well as “better charge/discharge profiles”. The EIS results also indicate that the ZnO doped SnSb-ZnO (2.5%) may be a potential anode material for Lithium-ion batteries, based on least impedance. The galvanostatic discharge and charge tests are in the pipeline. This study provides a logical and lucid direction for the efficient design of components and construction of the structures of composite anode materials such that significant improvement could be made to the implementation of Li-ion batteries.

REFRENCES

1. Nair, N. K. C., & Garimella, N. (2010). Battery energy storage systems: Assessment for small-scale renewable energy integration. *Energy and Buildings*, *42*(11), 2124-2130.

2. Pistoia, G. (2005). *Batteries for portable devices*. Elsevier.

3. Bellis, M. (2008). Biography of Alessandro Volta–Stored Electricity and the First Battery. *Google Scholar*.

4. Oakes, E. H. (2014). *A to Z of STS scientists*. Infobase Publishing.

5. Linden, D., & Reddy, T. B. (2002). Handbook of Batteries. 3rd. *McGraw-Hill*.

6. Olivetti, E., Gregory, J., & Kirchain, R. (2011). Life cycle impacts of alkaline batteries with a focus on end-of-life. *Study conducted for the National Electric Manufacturers Association*.

7. Hooper, A., & Sequeira, C. A. (Eds.). (1985). *Solid state batteries*. Martinus Nijhoff.

8. Linden, D. (2005). Batteries and Fuel Cells. *Electronics Engineers' Handbook." Edited by: DG Fink and AA McKenzie, McGraw-Hill Book Co., NY*, 7-66.

9. Nelson, R. F., & Kepros, M. A. (1999). AC ripple effects on VRLA batteries in float applications. In *Battery Conference on Applications and Advances, 1999. The Fourteenth Annual* (pp. 281-289). IEEE.

10. Buthelezi, T., Dingrando, L., Hainen, N., Wistrom, C., & Zike, D. (2008). *Chemistry: Matter and change*. Glencoe/McGraw-Hill.

11. Mauger, A., & Julien, C. M. (2017). Critical review on lithium-ion batteries: are they safe? Sustainable?. *Ionics*, *23*(8), 1933-1947.

12. Whittingham, M. S. (1976). Electrical energy storage and intercalation chemistry. *Science*, *192*(4244), 1126-1127.

13. Besenhard, J. O., & Eichinger, G. (1976). High energy density lithium cells: Part I. Electrolytes and anodes. *Journal of Electroanalytical Chemistry and Interfacial Electrochemistry*, *68*(1), 1-18.

14. Godshall, N. A. (1986). Lithium transport in ternary lithium-copper-oxygen cathode materials. *Solid State Ionics, 18*, 788-793.

15. Yazami, R., & Touzain, P. (1983). A reversible graphite-lithium negative electrode for electrochemical generators. *Journal of Power Sources*, *9*(3), 365-371.

16. Amatucci, G. G., Tarascon, J. M., & Klein, L. C. (1996). Coo2, the end member of the li x coo2 solid solution. *Journal of The Electrochemical Society*, *143*(3), 1114-1123.

17. Wakita, S., & Okae, I. (2008). *U.S. Patent Application No. 11/745,941*.

18. Murphy, D. W., & Trumbore, F. A. (1976). The Chemistry of TiS3 and NbSe3 Cathodes. *Journal of The Electrochemical Society*, *123*(7), 960-964.

19. Mizushima, K., Jones, P. C., Wiseman, P. J., & Goodenough, J. B. (1980). LixCoO2 (0< x<-1): A new cathode material for batteries of high energy density. *Materials Research Bulletin*, *15*(6), 783-789.

20. Zaghib, K., Julien, C. M., & Prakash, J. (Eds.). (2003). New Trends in Intercalation Compounds for Energy Storage and Conversion: Proceedings of the International Symposium. The Electrochemical Society.

21. Du Pasquier, A., Plitz, I., Menocal, S., & Amatucci, G. (2003). A comparative study of Li-ion battery, supercapacitor and nonaqueous asymmetric hybrid devices for automotive applications. *Journal of Power Sources*, *115*(1), 171-178.

22. Williard, N., He, W., Hendricks, C., & Pecht, M. (2013). Lessons learned from the 787 dreamliner issue on lithium-ion battery reliability. *Energies*, *6*(9), 4682-4695.

23. Jiang, J., Li, Y., Liu, J., Huang, X., Yuan, C., & Lou, X. W. D. (2012). Recent advances in metal oxide-based electrode architecture design for electrochemical energy storage. *Advanced materials*, *24*(38), 5166-5180.

24. Wang, Z., Zhou, L., & Lou, X. W. (2012). Metal oxide hollow nanostructures for lithium-ion batteries. *Advanced materials*, *24*(14), 1903-1911.

25. Prosini, P. P., Carewska, M., Loreti, S., Minarini, C., & Passerini, S. (2000). Lithium iron oxide as alternative anode for li-ion batteries. *International Journal of Inorganic Materials*, *2*(4), 365-370.

26. Bruce, P. G., Scrosati, B., & Tarascon, J. M. (2008). Nanomaterials for rechargeable lithium batteries. *Angewandte Chemie International Edition*, *47*(16), 2930-2946.

27. Capiglia, C., Saito, Y., Kataoka, H., Kodama, T., Quartarone, E., & Mustarelli, P. (2000). Structure and transport properties of polymer gel electrolytes based on PVdF-HFP and LiN (C2F5SO2) 2. *Solid State Ionics*, *131*(3-4), 291-299.

28. Li, H., & Zhou, H. (2012). Enhancing the performances of Li-ion batteries by carbon-coating: present and future. *Chemical Communications*, *48*(9), 1201-1217.

29. Aurbach, D. (2000). Review of selected electrode–solution interactions which determine the performance of Li and Li ion batteries. *Journal of Power Sources*, *89*(2), 206-218.

30. Park, T. H., Yeo, J. S., Seo, M. H., Miyawaki, J., Mochida, I., & Yoon, S. H. (2013). Enhancing the rate performance of graphite anodes through addition of natural

graphite/carbon nanofibers in lithium-ion batteries. *Electrochimica Acta*, *93*, 236-240.

31. Haik, O., Ganin, S., Gershinsky, G., Zinigrad, E., Markovsky, B., Aurbach, D., & Halalay, I. (2011). On the thermal behavior of lithium intercalated graphites. *Journal of The Electrochemical Society*, *158*(8), A913-A923.

32. Wang, H., Yoshio, M., Abe, T., & Ogumi, Z. (2002). Characterization of carbon-coated natural graphite as a lithium-ion battery anode material. *Journal of The Electrochemical Society*, *149*(4), A499-A503.

33. Nakagawa, H., Domi, Y., Doi, T., Ochida, M., Tsubouchi, S., Yamanaka, T., ... & Ogumi, Z. (2013). In situ Raman study on the structural degradation of a graphite composite negative-electrode and the influence of the salt in the electrolyte solution. *Journal of Power Sources*, *236*, 138-144.

34. Fujimoto, H., Tokumitsu, K., Mabuchi, A., Chinnasamy, N., & Kasuh, T. (2010). The anode performance of the hard carbon for the lithium ion battery derived from the oxygen-containing aromatic precursors. *Journal of Power Sources*, *195*(21), 7452-7456.

35. Yang, J., Zhou, X. Y., Li, J., Zou, Y. L., & Tang, J. J. (2012). Study of nano-porous hard carbons as anode materials for lithium ion batteries. *Materials Chemistry and Physics*, *135*(2-3), 445-450.

36. Bridges, C. A., Sun, X. G., Zhao, J., Paranthaman, M. P., & Dai, S. (2012). In situ observation of solid electrolyte interphase formation in ordered mesoporous hard carbon by small-angle neutron scattering. *The Journal of Physical Chemistry C*, *116*(14), 7701-7711.

37. Yu, Y., Cui, C., Qian, W., Xie, Q., Zheng, C., Kong, C., & Wei, F. (2013). Carbon nanotube production and application in energy storage. *Asia-Pacific Journal of Chemical Engineering*, *8*(2), 234-245.

38. Liang, M., & Zhi, L. (2009). Graphene-based electrode materials for rechargeable lithium batteries. *Journal of Materials Chemistry*, *19*(33), 5871-5878.

39. Moretti, A., Kim, G. T., Bresser, D., Renger, K., Paillard, E., Marassi, R., ... & Passerini, S. (2013). Investigation of different binding agents for nanocrystalline anatase TiO2 anodes and its application in a novel, green lithium-ion battery. *Journal of Power Sources*, *221*, 419-426.

40. Wu, F., Wang, Z., Li, X., Guo, H., Yue, P., Xiong, X., ... & Zhang, Q. (2012). Characterization of spherical-shaped Li4Ti5O12 prepared by spray drying. *Electrochimica Acta*, *78*, 331-339.

41. Reddy, A. L. M., Gowda, S. R., Shaijumon, M. M., & Ajayan, P. M. (2012). Hybrid nanostructures for energy storage applications. *Advanced materials*, *24*(37), 5045-5064.
42. Gu, J., Collins, S. M., Carim, A. I., Hao, X., Bartlett, B. M., & Maldonado, S. (2012). Template-Free Preparation of Crystalline Ge Nanowire Film Electrodes via an Electrochemical Liquid–Liquid–Solid Process in Water at Ambient Pressure and Temperature for Energy Storage. *Nano letters*, *12*(9), 4617-4623.

43. Szczech, J. R., & Jin, S. (2011). Nanostructured silicon for high capacity lithium battery anodes. *Energy & Environmental Science*, *4*(1), 56-72.

44. Chandrasekaran, R., Magasinski, A., Yushin, G., & Fuller, T. F. (2010). Analysis of lithium insertion/deinsertion in a silicon electrode particle at room temperature. *Journal of the Electrochemical Society*, *157*(10), A1139-A1151.

45. Li, X., & Wang, C. (2013). Engineering nanostructured anodes via electrostatic spray deposition for high performance lithium ion battery application. *Journal of Materials Chemistry A*, *1*(2), 165-182.

46. Kim, H., & Cho, J. (2008). Hard templating synthesis of mesoporous and nanowire SnO 2 lithium battery anode materials. *Journal of Materials Chemistry*, *18*(7), 771-775.

47. Yang, Z., Du, G., Guo, Z., Yu, X., Li, S., Chen, Z., ... & Liu, H. (2010). Plum-branch-like carbon nanofibers decorated with SnO 2 nanocrystals. *Nanoscale*, *2*(6), 1011-1017.

48. Shen, L., Yuan, C., Luo, H., Zhang, X., Xu, K., & Xia, Y. (2010). Facile synthesis of hierarchically porous Li 4 Ti 5 O 12 microspheres for high rate lithium ion batteries. *Journal of Materials Chemistry*, *20*(33), 6998-7004.

49. Wang, B., Chen, J. S., Wu, H. B., Wang, Z., & Lou, X. W. (2011). Quasiemulsion-templated formation of α-Fe2O3 hollow spheres with enhanced lithium storage properties. *Journal of the American Chemical Society*, *133*(43), 17146-17148.

50. Zhang, L., Hu, P., Zhao, X., Tian, R., Zou, R., & Xia, D. (2011). Controllable synthesis of core–shell Co@ CoO nanocomposites with a superior performance as an anode material for lithium-ion batteries. *Journal of Materials Chemistry*, *21*(45), 18279-18283.

51. Stan, M. C., Klöpsch, R., Bhaskar, A., Li, J., Passerini, S., & Winter, M. (2013). Cu3P Binary Phosphide: Synthesis via a Wet Mechanochemical Method and Electrochemical Behavior as Negative Electrode Material for Lithium-Ion Batteries. *Advanced Energy Materials*, *3*(2), 231-238.

52. Soto, F. A., Ma, Y., Martinez de la Hoz, J. M., Seminario, J. M., & Balbuena, P. B. (2015). Formation and growth mechanisms of solid-electrolyte interphase layers in rechargeable batteries. *Chemistry of Materials*, *27*(23), 7990-8000.

53. Panitz, J. C., Wietelmann, U., & Scholl, M. (2007). *U.S. Patent No. 7,226,704*. Washington, DC: U.S. Patent and Trademark Office.

54. Venugopal, G., Moore, J., Howard, J., & Pendalwar, S. (1999). Characterization of microporous separators for lithium-ion batteries. *Journal of Power Sources*, *77*(1), 34-41.

55. Besenhard, J. O., Yang, J., & Winter, M. (1997). Will advanced lithium-alloy anodes have a chance in lithium-ion batteries?. *Journal of Power Sources*, *68*(1), 87-90.

56. McDowall, J., Biensan, P., & Broussely, M. (2007, September). Industrial lithium ion battery safety-what are the tradeoffs?. In *Telecommunications Energy Conference, 2007. INTELEC 2007. 29th International* (pp. 701-707). IEEE.

57. Yang, J., Winter, M., & Besenhard, J. O. (1996). Small particle size multiphase Li-alloy anodes for lithium-ionbatteries. *Solid State Ionics*, *90*(1-4), 281-287.

58. Wang, Y., & Lee, J. Y. (2006). One-Step, Confined Growth of Bimetallic Tin–Antimony Nanorods in Carbon Nanotubes Grown In Situ for Reversible Li+ Ion Storage. *Angewandte Chemie International Edition*, *45*(42), 7039-7042.

59. Wang, Z., Tian, W., & Li, X. (2007). Synthesis and electrochemistry properties of Sn–Sb ultrafine particles as anode of lithium-ion batteries. *Journal of alloys and compounds*, *439*(1-2), 350-354.

60. Wang, Y., Djerdj, I., Smarsly, B., & Antonietti, M. (2009). Antimony-doped SnO2 nanopowders with high crystallinity for lithium-ion battery electrode. *Chemistry of Materials*, *21*(14), 3202-3209.

61. Li, H., Wang, Z., Chen, L., & Huang, X. (2009). Research on advanced materials for Li-ion batteries. *Advanced materials*, *21*(45), 4593-4607.

62. Chen, S., Chen, P., Wu, M., Pan, D., & Wang, Y. (2010). Graphene supported Sn–Sb@ carbon core-shell particles as a superior anode for lithium ion batteries. *Electrochemistry Communications*, *12*(10), 1302-1306.

63. Zhang, W. J. (2011). A review of the electrochemical performance of alloy anodes for lithium-ion batteries. *Journal of Power Sources*, *196*(1), 13-24.

64. Kamali, A. R., & Fray, D. J. (2011). Tin-based materials as advanced anode materials for lithium ion batteries: a review. *Rev. Adv. Mater. Sci*, *27*(1), 14-24.

65. Park, C. M., & Jeon, K. J. (2011). Porous structured SnSb/C nanocomposites for Li-ion battery anodes. *Chemical Communications*, *47*(7), 2122-2124.

66. Xie, J., Song, W., Zheng, Y., Liu, S., Zhu, T., Cao, G., & Zhao, X. (2011). Preparation and Li-storage properties of SnSb/graphene hybrid nanostructure by a facile one-step solvothermal route. *International Journal of Smart and Nano Materials*, *2*(4), 261-271.

67. Nitta, N., & Yushin, G. (2014). High-capacity anode materials for lithium-ion batteries: choice of elements and structures for active particles. *Particle & Particle Systems Characterization*, *31*(3), 317-336.

68. Goriparti, S., Miele, E., De Angelis, F., Di Fabrizio, E., Zaccaria, R. P., & Capiglia, C. (2014). Review on recent progress of nanostructured anode materials for Li-ion batteries. *Journal of Power Sources*, *257*, 421-443.

69. Nithyadharseni, P., Reddy, M. V., Nalini, B., Kalpana, M., & Chowdari, B. V. (2015). Sn-based intermetallic alloy anode materials for the application of lithium ion batteries. *Electrochimica Acta*, *161*, 261-268.

70. Ren, X., Cai, H., Zhang, W., Li, Y., Zhang, P., Deng, L., & Sun, L. (2016). SnSbCux Alloy Composite Anode Materials for High Performance Lithium-Ion Batteries. *INTERNATIONAL JOURNAL OF ELECTROCHEMICAL SCIENCE*, *11*(11), 9508-9518.

71. Chen, X., Ru, Q., Wang, Z., Hou, X., & Hu, S. (2017). Ternary Sn-Sb-Co alloy particles embedded in reduced graphene oxide as lithium ion battery anodes. *Materials Letters*, *191*, 218-221.

72. Sengupta, S., Patra, A., Akhtar, M., Das, K., Majumder, S. B., & Das, S. (2017). 3D microporous Sn-Sb-Ni alloy impregnated Ni foam as high-performance negative electrode for lithium-ion batteries. *Journal of Alloys and Compounds*, *705*, 290-300.

73. Yi, Z., Han, Q., Geng, D., Wu, Y., Cheng, Y., & Wang, L. (2017). One-pot chemical route for morphology-controllable fabrication of Sn-Sb micro/nano-structures: Advanced anode materials for lithium and sodium storage. *Journal of Power Sources*, *342*, 861-871.

74. Eftekhari, A. (2017). Low voltage anode materials for lithium-ion batteries. *Energy Storage Materials*, *7*, 157-180.

75. Qi, W., Shapter, J. G., Wu, Q., Yin, T., Gao, G., & Cui, D. (2017). Nanostructured anode materials for lithium-ion batteries: principle, recent progress and future perspectives. *Journal of Materials Chemistry A*, *5*(37), 19521-19540.

76. Das, S., Guru Row, T. N., & Bhattacharyya, A. J. (2017). Probing the Critical Role of Sn Content in SnSb@ C Nanofiber Anode on Li Storage Mechanism and Battery Performance. *ACS Omega*, *2*(12), 9250-9260.

77. Arico, A. S., Bruce, P., Scrosati, B., Tarascon, J. M., & Van Schalkwijk, W. (2005). Nanostructured materials for advanced energy conversion and storage devices. *Nature materials*, *4*(5), 366.

78. Larcher, D., Beattie, S., Morcrette, M., Edstroem, K., Jumas, J. C., & Tarascon, J. M. (2007). Recent findings and prospects in the field of pure metals as negative electrodes for Li-ion batteries. *Journal of Materials Chemistry*, *17*(36), 3759-3772.

79. Rönnebro, E., Yin, J., Kitano, A., Wada, M., Tanase, S., & Sakai, T. (2004). Structural analysis by synchrotron XRD of a Ag52Sn48 nanocomposite electrode for advanced Li-ion batteries. *Journal of the Electrochemical Society*, *151*(10), A1738-A1744.

80. Courtney, I. A., & Dahn, J. R. (1997). Electrochemical and in situ X-ray diffraction studies of the reaction of lithium with tin oxide composites. *Journal of the Electrochemical Society*, *144*(6), 2045-2052.

81. Fleischauer, M. D., Obrovac, M. N., McGraw, J. D., Dunlap, R. A., Topple, J. M., & Dahn, J. R. (2006). Al-M (M= Cr, Fe, Mn, Ni) thin-film negative electrode materials. *Journal of The Electrochemical Society*, *153*(3), A484-A491.

82. Yang, J., Takeda, Y., Imanishi, N., Xie, J. Y., & Yamamoto, O. (2000). Intermetallic SnSbx compounds for lithium insertion hosts. *Solid State Ionics*, *133*(3-4), 189-194.

83. Si, Q., Hanai, K., Imanishi, N., Kubo, M., Hirano, A., Takeda, Y., & Yamamoto, O. (2009). Highly reversible carbon–nano-silicon composite anodes for lithium rechargeable batteries. *Journal of Power Sources*, *189*(1), 761-765.

84. Trahey, L., Vaughey, J. T., Kung, H. H., & Thackeray, M. M. (2009). High-capacity, microporous Cu6Sn5–Sn anodes for Li-ion batteries. *Journal of The Electrochemical Society*, *156*(5), A385-A389.

85. Park, C. M., & Sohn, H. J. (2009). A mechano-and electrochemically controlled SnSb/C nanocomposite for rechargeable Li-ion batteries. *Electrochimica Acta*, *54*(26), 6367-6373.

86. Tostmann, H., Kropf, A. J., Johnson, C. S., Vaughey, J. T., & Thackeray, M. M. (2002). In situ x-ray absorption studies of electrochemically induced phase changes in lithium-doped InSb. *Physical Review B*, *66*(1), 014106.

87. Kim, J. B., Lee, H. Y., Lee, K. S., Lim, S. H., & Lee, S. M. (2003). Fe/Si multi-layer thin film anodes for lithium rechargeable thin film batteries. *Electrochemistry communications*, *5*(7), 544-548.

88. Jung, H., Park, M., Yoon, Y. G., Kim, G. B., & Joo, S. K. (2003). Amorphous silicon anode for lithium-ion rechargeable batteries. *Journal of power sources*, *115*(2), 346-351.

89. Chen, Z., Christensen, L., & Dahn, J. R. (2003). Large-volume-change electrodes for Li-ion batteries of amorphous alloy particles held by elastomeric tethers. *Electrochemistry communications*, *5*(11), 919-923.

90. Whittig, L. D., & Allardice, W. R. (1986). X-ray diffraction techniques. *Methods of Soil Analysis: Part 1—Physical and Mineralogical Methods*, (methodsofsoilan1), 331-362.

91. Ewald P.P. (1962) The Principles of X-ray Diffraction. In: Ewald P.P. (eds) Fifty Years of X-Ray Diffraction. Springer, Boston, MA

92. Cullity, B. D. (2001). Elements of X-ray Diffraction.

93. Khursheed, A. (2007). *U.S. Patent No. 7,294,834*. Washington, DC: U.S. Patent and Trademark Office.

94. Todokoro, H., & Ezumi, M. (1999). *U.S. Patent No. 5,872,358*. Washington, DC: U.S. Patent and Trademark Office.

95. Joy, D. C. (2006). Scanning electron microscopy. *Materials Science and Technology*.

96. Chepyala, S. (2017). *Simulation Of Li-Ion Coin Cells Using Comsol Multiphysics* (Doctoral dissertation, The Florida State University).

97. Purkayastha, R. T., & McMeeking, R. M. (2012). An integrated 2-D model of a lithium ion battery: the effect of material parameters and morphology on storage particle stress. *Computational Mechanics*, *50*(2), 209-227.